Title

AAPM task group report 135.B: Quality assurance for robotic radiosurgery

Authors

Wang, Lei

Descovich, Martina

Wilcox, Ellen E

et al.

Publication Date

2024-10-25

DOI

10.1002/mp.17478

Peer reviewed

Received: 26 September 2023 | Revised: 31 July 2024 | Accepted: 26 September 2024

DOI: 10.1002/mp.17478

AAPM SCIENTIFIC REPORT

MEDICAL PHYSICS

AAPM task group report 135.B: Quality assurance for robotic radiosurgery

Lei Wang[1] | **Martina Descovich**[2] | **Ellen E. Wilcox**[3] | **Jun Yang**[4] | **Alan B. Cohen**[5] | **Christoph Fuerweger**[6] | **Anand Prabhu**[7] | **Jeffrey A. Garrett**[8] | **David D. Taylor Jr.**[9] | **Matt Noll**[10] | **Sonja Dieterich**[11]

[1]Stanford University School of Medicine, Stanford, California, USA

[2]University of California San Francisco, San Francisco, California, USA

[3]Vancouver, British Columbia, Canada

[4]ChanCheng Hospital, Foshan, Guangdong, China

[5]GenesisCare USA, Inc., Yellville, Arkansas, USA

[6]European Radiosurgery Center Munich, München, Germany

[7]Riverview Medical Center (Hackensack Meridian Health), Red Bank, New Jersey, USA

[8]Varian Advanced Oncology Services, Palo Alto, California, USA

[9]Grand Junction, Colorado, USA

[10]Accuray Inc., Sunnyvale, California, USA

[11]UC Davis Medical Center, Sacramento, California, USA

Correspondence
Lei Wang, Stanford University School of Medicine, Stanford, CA 94304, USA.
Email: LeiWang@stanford.edu

Abstract

AAPM Task Group Report 135.B covers new technology components that have been added to an established radiosurgery platform and updates the components that were not well covered in the previous report. Considering the current state of the platform, this task group (TG) is a combination of a foundational task group to establish the basis for new processes/technology and an educational task group updating guidelines on the established components of the platform. Because the technology discussed in this document has a relatively small user base compared to C-arm isocentric linacs, the authors chose to emphasize the educational components to assist medical physicists who are new to the technology and have not had the opportunity to receive in-depth vendor training at the time of reading this report. The TG has developed codes of practice, introduced QA, and developed guidelines which are generally expected to become enduring practice. This report makes prescriptive recommendations as there has not been enough longitudinal experience with some of the new technical components to develop a data-based risk analysis.

KEYWORDS

image guided SRS, image guided SBRT, robotic radio-surgery

1 | INTRODUCTION

1.1 | Charges

TG 135.B serves as an addendum to the original TG 135,[1] therefore we carry on the charges of the original TG 135[1]:

1. To make recommendations on a code of practice for Robotic Radiosurgery Quality Assurance (QA).
2. To make recommendations on quality assurance and dosimetric verification techniques, especially in regards to the real-time respiratory motion tracking software.
3. To make recommendations on issues which require further research and development.

1.2 | Type of task group

AAPM TG 135.B covers new technology components that have been added to an established radiosurgery platform and updates the components that were not well covered in the previous report. Considering the

current state of the platform, this task group (TG) is a combination of a foundational task group to establish the basis for new processes/technology and an educational task group updating guidelines on the established components of the platform. Because the technology discussed in this document has a relatively small user base compared to C-arm isocentric linacs, the authors chose to emphasize the educational components to assist medical physicists who are new to the technology and have not had the opportunity to receive in-depth vendor training at the time of reading this report. The TG has developed codes of practice, introduced QA, and developed guidelines which are generally expected to become enduring practice. This report makes prescriptive recommendations as there has not been enough longitudinal experience with some of the new technical components to develop a data-based risk analysis.

1.3 | Changes in technology since the original AAPM TG 135 report

The original TG 135 Report,[1] published in 2011, covered the basic CyberKnife QA components extensively. This included: radiation shielding, security, beam QA, imaging components, targeting accuracy, etc. as well as providing daily, monthly, and annual QA recommendations. Since then, several new technologies were introduced which required significant changes to the QA approach. With respect to hardware, the Iris collimator[2] was introduced in early 2008 and was followed in 2014 by a multi-leaf collimator (MLC).[3,4] Neither of these were included in the previous report. For image-guidance, a new lung tracking algorithm was introduced which enabled various tracking modules dependent on the location and visibility of the tumors on the stereoscopic x-ray images. The Monte-Carlo (MC) algorithm was discussed briefly in the previous report but lacked detailed guidance in commissioning and QA. The Synchrony motion tracking system also had significant improvements, necessitating an update to QA recommendations and algorithm description. Table 1 shows a summary of the three representative CyberKnife models.[5]

1.4 | Scope of TG 135.B

This task group will focus on (1) the newly introduced Iris (Section 2) and MLC (Section 3) collimation systems and their quality assurance; (2) Quality Control (QC) and QA of motion management with Synchrony (Section 4) and lung optimized treatment (LOT) workflow (Sections 4 and 5); (3) commissioning and QA recommendations of the MC calculation (Section 6). TG 135.B does not intend to replace the original TG 135 Report[1] since the basics of the CyberKnife system have not changed. The basic system description and QA recommendations that are included in TG 135 will not be duplicated in this report nor will the task group cover the software advances that have no direct impact on the QA practice, such as the integrated patient database system (IDMS) and the updates of the treatment planning system (The Multiplan treatment planning system was replaced by the Precision treatment planning system in 2017). For treament planning system QA, we refer to TG 53 (Quality assurance for clinical radiotherapy treatment planning)[6] and MPPG 5.a/MPPG 5.b (Commissioning and QA of Treatment Planning Dose Calculations—Megavoltage Photon and Electron Beams).[7,8] A detailed discussion of commissioning procedures and beam data measurements for small radiation fields will not be provided as this has been extensively covered in IAEA Report 483,[9] TG 155,[10] and the manufacturer provided PEG.[11] However, QA recommendations related to commissioning and beam QA will be provided. Finally, updated QA recommendations will be combined with those from the previous TG 135 report and a summary of recommendations will be given in Section 7.

1.5 | Definitions

Most of the following definitions have been introduced in the previous TG 135 Report.[1] For the convenience of the readers, we list all the definitions that appear in this document.

AQA : "Auto QA," a Robot targeting test: The centering of a radiographic shadow of a 2 cm diameter tungsten ball hidden in a cubic phantom is measured on a pair of orthogonal films. A detailed discussion can be found in the original TG 135.

CAX: Central axis representing the centerline of the radiation beam.

DQA: Delivery Quality Assurance: The DQA plan is an overlay of a patient plan on a phantom. The plan is delivered and the measured dose in the phantom can be compared with the calculated dose for quality assurance, typically by using a gamma-index pass/fail criteria. The DQA assesses both spatial and dosimetric accuracy of delivery, and is the most comprehensive, overall assessment of the system.

E2E: End-to-End test: A phantom containing a hidden target and orthogonal films is taken from simulation through treatment delivery. Targeting accuracy is quantified as the difference between the center of the dose distribution (70% isodose line is often used) measured on the film and the geometrical center of the target. The E2E test is performed using an isocentric

TABLE 1 Technical specifications of three representative CyberKnife® models.

	CyberKnife circa 1997–1999	CyberKnife VSI 2009	CyberKnife M6/S7 2012/2020
Robotic manipulator type and precision	FANUC robot 0.5 mm precision	KUKA KR 240 robot 0.12 mm precision	KUKA KR 300 R2500 ultra robot 0.12 mm precision
Beam collimation	Fixed circular collimators	Fixed circular collimators Iris variable aperture collimator	Fixed circular collimators Iris variable aperture collimator InCise Multileaf Collimator (2014)
Image registration and tracking methods	Skull skeletal tracking with 3D translation corrections	Skull skeletal tracking with 6D translation and rotation corrections Spine skeletal tracking with 6D corrections Fiducial marker tracking with 6D corrections Lung tumor tracking based on tumor: lung radiographic contrast with 3D corrections	Skull skeletal tracking with 6D translation and rotation corrections Spine skeletal tracking with 6D corrections Fiducial marker tracking with 6D corrections Lung tumor tracking based on tumor: lung radiographic contrast with 3D corrections
Real time respiratory motion tracking		Synchrony with fiducial and lung tumor tracking	Synchrony with fiducial, lung and spine prone tracking.
Overall targeting accuracy (static target)	Mean: 1.6 mm. Range: 0.6–2.5 mm[24] E2E in phantom	Spec: ≤0.95 mm E2E in phantom	Spec: ≤0.95 mm E2E in phantom
Overall targeting accuracy (target undergoing respiratory motion)	n/a	Spec: ≤1.5 mm (v9.6 and before) ≤0.95 mm (v10.0 and after) E2E in phantom	Spec: ≤1.5 mm (v9.6 and before) ≤0.95 mm (v10.0 and after) E2E in phantom
Dose rate	300 MU/min	600–1000 MU/min	1000 MU/min or 800 MU/min
Image detectors	Gadolinium oxysulfide fluoroscopes with pixel size 1.25×1.25 mm^2	Amorphous silicon flat panel detectors with pixel size 0.4×0.4 mm^2	Amorphous silicon flat panel detectors with pixel size 0.4×0.4 mm^2
Dose calculation algorithm(s)	Ray Tracing	Monte-Carlo Ray Tracing	Monte-Carlo Ray Tracing FSPB
Patient positioning system	Manually operated treatment couch	Fully integrated 5-DOF standard treatment couch with manual yaw adjustment Fully integrated 6-DOF robotic couch Patient Positioning System (option) Fully integrated 7-DOF robotic couch with seated load (option). The 7th DOF is knee up position option.	Fully integrated 5-DOF standard treatment couch with manual yaw adjustment Fully integrated 6-DOF robotic couch Patient Positioning System (option)
Clinical applications	Intracranial and upper spine radiosurgery (under FDA Investigational Device Exemption)	Anywhere in the body where radiosurgery is clinically indicated (with FDA 510(k) regulatory clearance).	Anywhere in the body where radiosurgery is clinically indicated (with FDA 510(k) regulatory clearance).

The targeting accuracy for the 1997–1999 model is reported by Murphy et al. in 1996. All other targeting accuracy information is from manufacturer's specification.

treatment plan. Its purpose is to be a sophisticated Winston–Lutz test, checking spatial delivery accuracy together with tracking modality accuracy. Unlike the DQA test, the E2E does not have a patient-specific dosimetry component. A detailed discussion can be found in the original TG 135.

EMO: Emergency Motion Off.
EPO: Emergency Power Off.
FC/FCA: Fixed collimator/Fixed collimator assembly.
FWHM: Full width at half maximum.
Iris: A variable aperture collimation system designed to simulate the 12 fixed circular cones.
IQA: Iris QA.
LOT: Lung Optimized Treatment.
MC: Monte Carlo.
MU: Monitor Unit.
MLC: Multi leaf collimator.

OCR: Off-center ratio.
OF: Output Factor.
PDD: Percentage Depth Dose.
PEG: Physics Essentials Guide, Accuray Inc., Sunnyvale, CA
QA: Quality assurance.
QC: Quality control.
SRS: Stereotactic radiosurgery (including stereotactic radiotherapy, SRT).
SBRT: Stereotactic body radiosurgery
SAD: Source-to-axis distance.
TPR: Tissue-Phantom Ratio.
TG: Task Group.
Xsight Spine tracking: A fiducial less tracking mode that directly tracks using spine bony anatomy.
Xsight Lung tracking: A fiducial less tracking mode that directly tracks on tumor.

2 | CYBERKNIFE IRIS COLLIMATION SUBSYSTEM

2.1 | Introduction

In 2008, Accuray, Inc. introduced the Iris variable collimation system[2] for the CyberKnife (Accuray, Inc., Sunnyvale, CA, USA), together with an automated collimator exchange system (Xchange). The underlying motivation for the Iris and Xchange products is to relieve the therapists from manually exchanging the heavy tungsten fixed cones and to support flexible use of multiple field sizes. As a consequence, dose distributions of irregular shape could potentially be produced in a more time-efficient manner. The Iris collimator is clinically available for CyberKnife versions G4, VSI, M6, and S7. There are currently three generations of the Iris collimation system. The original version was introduced in 2008, with updates in 2011 (v2), and 2013 (v3). The following description and recommendations are applicable to all versions of Iris and Xchange, unless stated otherwise.

2.2 | Collimation assembly physical description

To accommodate the existing fixed cones and the newer variable collimation system, a significant re-engineering of the CyberKnife accelerator beam delivery structure was required. Separate collimation subassemblies were created: one for the existing fixed collimators (FCA—fixed collimator assembly), one containing the Iris variable collimation system, and one for the MLC collimation system (discussed later).

Because the collimation subassemblies are too heavy to be manually exchanged, this function is performed by the robot manipulator using an automated exchange function. An exchange table contains receptacle storage positions for the fixed and variable collimation subassemblies. Different versions of this table are in use today (Figure 1). Earlier tables (Figure 1a) include storage positions for FCA, Iris, and all twelve fixed cones on top of the table, allowing for exchange of the subassemblies and automated pick-up of individual fixed cones. The most recent table for the CyberKnife M6 and S7 generation was designed to include a third subassembly containing an MLC, but requires the manual exchange of individual fixed cones due to spatial limitations (Figure 1b).

During CyberKnife installation, the exact location of all the exchangeable collimation components is established using an automated calibration process that utilizes the accelerator treatment beam central axis (CAX) centerline laser.

The ongoing stability and validity of the exchange table position calibration is monitored by several optical sensors. Depending on the table version, these can be located on the front of the exchange table, at the mechanical center of each storage position of the collimator subassemblies, or at the storage positions for all 12 fixed collimator cones. When an exchange process is initiated, the robot points the centerline laser at the table position optical sensor. If, for whatever reason, this sensor does not produce a signal of sufficient amplitude, the exchange process is interrupted and the CyberKnife system is interlocked.

The integrity of the optical exchange position verification process can be compromised by uncertainties in the position of the exchange table, the position and output of the centerline laser, the mechanical condition of the accelerator head, and foreign objects (e.g., dust) in the optical path. As such, the exchange process also serves as an indirect QA check of geometric consistency of the robot position, linac head, and laser. The failure of a component exchange will require an evaluation by a service engineer to identify the root cause.

2.3 | Collimation subassembly mechanical alignment

Geometric calibration of the CyberKnife system is achieved by using a beam centerline laser as a surrogate for the radiation beam centerline.[1] Therefore, one of the key elements for geometric integrity is the alignment of the centerline laser beam with the radiation beam CAX. On the CyberKnife, the electron target, primary collimator, centerline laser assembly, and the "tool changer" assembly are all mechanically fixed to the

FIGURE 1 Different configurations of the CK Xchange table: G4/VSI (a) with receptacle storage positions for the FCA, Iris, and M6/S7 (b) with receptacles for MLC, FCA, and Iris (from left to right). The M6/S7 Xchange table holds the 12 fixed cones on the side of the table and must be changed manually during treatment.

linear accelerator structure. Barring a catastrophic collision these elements should never change their relative positions with respect to each other. The only adjustment that can be made is in the position and direction of the laser beam emitted from the centerline laser assembly, which is designed such that the effective source position and angle of the centerline laser can be tuned. Because the laser is used for robot path calibration, any offset between the laser and the FCA, Iris and MLC centers will cause a consequent blurring of the high dose gradient regions, which is not compensated for by other calibration measures.[1] Therefore, it is most important that the actual position of the centerline laser with respect to the center of the radiation field be independently verified for all installed collimator assemblies before commissioning and robot path calibration (see original TG 135[1]). The original task group report recommended that the radial offset should not exceed 0.5 mm at 80 cm from the radiation source.[1] At that time, CyberKnife had only one fixed collimator system. The incorporation of multiple collimator subassemblies introduced additional small uncertainties in the laser to radiation alignment, which makes the 0.5 mm tolerance at 80 cm more difficult to achieve for all the collimators. Due to the fact that the laser alignment directly impacts the accuracy of the path calibration/verification, we strongly encourage the CAX alignment to be 0.5 mm at 80 cm and 1.0 mm at 160 cm for all collimators. If this tolerance is not achievable in some systems, we recommend the laser be best aligned with FCA (<0.5 mm at 80 cm) considering that the fixed collimators are usually used for the smallest targets where path calibration accuracy could cause the most significant impact on penumbra, and <1.0 mm at 80 cm for Iris and MLC which is the manufacturer's specification. The laser/radiation CAX coincidences should be checked before commissioning, path calibration, and quarterly. As with the FCA, exposure of radiochromic film with marked laser position can be used for the Iris and MLC collimators as well.

In clinical operation, the centerline laser is pointed at a fixed optical sensor (located either on the exchange table or the robot base, depending on the specific system configuration) at the start of each treatment. The intensity reading of the sensor is expected to exceed a predefined threshold. This pretreatment "laser alignment check" is an automated QA procedure intended to verify the geometric integrity of the robotic subsystem and inherently assumes stability of the laser position.

CyberKnife path calibrations and delta-man corrections[1] are performed independently for each collimator subassembly to account for the impact from different collimator assembly weights. Independent AQA and E2E tests with all collimators should be performed to maintain geometric integrity. The concept of AQA and E2E using Iris or MLC is identical to that for fixed cones, which is described in detail in the previous TG 135 Report.[1] Iris AQA tests should be performed in daily rotation with fixed cones and the MLC. E2E tests using Iris should be performed for all available tracking modes as part of commissioning, and selectively in monthly alternation with fixed cones and MLC depending on their clinical usage (see Section 7.2 for recommendation on alternation strategy).

2.4 | Iris technical description

2.4.1 | Variable collimation subassembly

Echner et al.[2] published a detailed description of the physical design of the Iris collimation system. This Task Group is providing a general descriptive overview of the

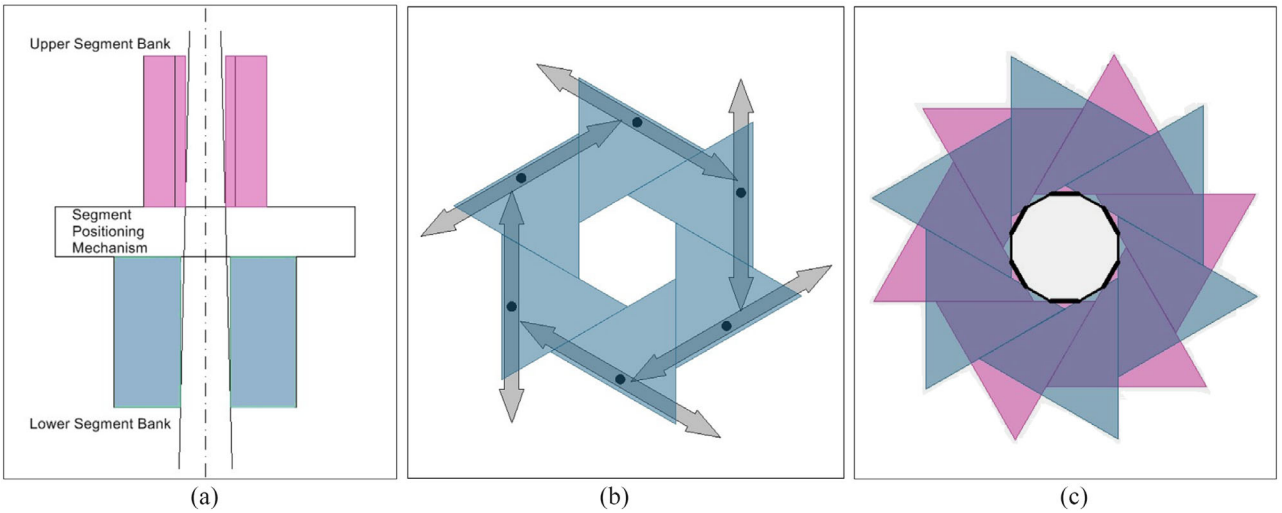

FIGURE 2 (a) Iris Collimator Segments—side view cross-section showing segment geometry and collimated beam boundary. (b) Iris Lower Collimating Segment Bank—arrows show the direction of movement of each of the triangular cross-section collimating segments. (c) Upper and Lower Iris Collimating segments as projected from the position of the radiation source. The inner dodecagon shape with variable line widths schematically represents the alternating beam penumbra widths produced at the treatment distance.

Iris system with emphasis on those characteristics that will have impact on, and/or require special attention in a QA program.

The variable aperture of the Iris collimation system is formed by two stacked banks (upper and lower) of six triangular collimator segments shown in Figure 2a. Each bank is configured to produce a hexagonal opening as shown schematically in Figure 2b. Each Tungsten alloy collimator segment is mounted on a linear bearing that moves in the direction shown. Individual segments cannot move independently because of mechanical interference with both neighbors.

Both banks of collimator segments are indexed to a single cam plate located between the collimator segment banks. The cam plate contains slots that engage a dedicated guide pin and bearing attached to each collimator segment carriage. A single drive motor rotates the cam plate that in turn positions all segments as a unit. This, in combination with the segment interference described above, provides a measure of confidence that segments cannot be individually out of place unless there has been a catastrophic mechanical failure. The two six-segment non-diverging collimator banks are positioned one above the other as shown in Figure 2a. The two banks are rotated 30° with respect to each other such that collimator segments of the opposite bank cover the inter-segment space of the other bank (Figure 2c).

2.4.2 | Iris collimator sizing

To monitor and control field size, the positions of two lower-bank collimator segments are continuously measured by two independent, temperature stabilized linear position sensors (differential variable reluctance transducers—DVRTs). The stack up of mechanical and sensor tolerances support a repeatability of 0.1 mm at the device, or 0.2 mm at the nominal treatment distance of 80 cm.[2,11] As of this writing, the available nominal field sizes are limited to those of the fixed collimators to allow for the use of the same treatment planning algorithm.

2.4.3 | Iris calibrations and initializations

Power is made available to the Iris components when the robot manipulator picks up the Iris collimator subassembly. A temperature control and heating system then maintains a tightly controlled temperature of 30°C for the DVRTs to ensure accurate and stable readings. The software enforces a warm-up period of 2–3 min before allowing initialization or field size changes. Iris is calibrated by the manufacturer by recording DVRT readings versus microswitch activation (two endpoint switches for Iris v1 and an additional switch in the middle for Iris v2/v3). This reference table is used by the DVRTs to determine the Iris field sizes.

Before delivery of an Iris treatment plan or before sizing the aperture in physics mode, initialization of the device is forced by the software. In this process, all microswitches are again sampled several times. For Iris v1, results are simply compared to the calibration reference, issuing an interlock in case of deviations. For Iris v2 and v3, this process is utilized to create a new set of up-to-date DVRT reference values for all field sizes which will be employed until the next initialization, where they are again overwritten. The purpose of this procedure is to fine-tune field sizes on a daily basis. For safety reasons, these short-term reference values

are compared to long-term baseline values established during Iris calibration, triggering a system interlock, and failing initialization in case of inconsistencies. In this manner, initialization is allowed to introduce small corrections to the Iris field sizes, but prohibits violating the integrity of calibration.

2.5 | Iris independent field size verification

The manufacturer's performance specification for reproducing aperture size to an accuracy of 0.2 mm at 80 cm SAD is dependent on the hardware that tells the calibration system when the collimator has reached the full open and full closed positions. Causes for failed Iris initialization may include segment position sensor component failure, temperature instability, end point dimension changes, mechanical interference among moving components, motor failure, component wear, etc. In some cases, it may be possible to recalibrate the Iris system. An independent verification of the Iris field sizes must be undertaken to demonstrate that the field sizes produced after a new Iris calibration are the same as those measured at the time of Iris beam commissioning. As there is no absolute field size specification from the manufacturer, each Iris can have different radiation field sizes compared to the nominal field sizes. The gold standard for this test is the same measurement method that produced the beam profile data at the time of commissioning, i.e., scanning a subset of beams in a water tank. As this is very time-consuming other methods have been developed by users as outlined in Section 2.5.2.

2.5.1 | Iris field sizing tolerances

The establishment of the magnitude of field sizing tolerances depends on two physical factors for the Iris collimator. A change in actual field size alters the radial distance from the CAX to the penumbra (OCR), and the OF, which is most pronounced for the smallest fields. Figure 3 shows sample output factors for Iris v2 and v3 as measured on two different CyberKnife systems. Error bars indicate the estimated range of measured values due to a change in field diameter by ±0.2 mm.

The impact of Iris field size variation needs to be viewed with some perspective. Firstly, the dodecagon shape of the Iris field (Figure 2c) has a maximum to minimum field size ratio within the shape of a single field of 1.035 (e.g., distances of 20.47 mm point-to-point vs. 19.77 mm face-to-face for a nominal field size of 20 mm). This individual field edge position uncertainty is averaged over all the beam entry directions to form the average edge position. Secondly, field size reproduction after recalibration or in a single QA measurement cannot be expected to be better than the specified

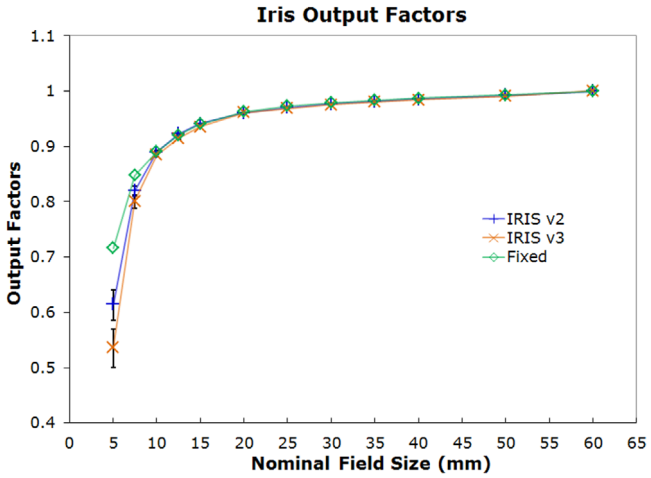

FIGURE 3 Sample Output Factors for Iris v2 and v3 as measured on two different CyberKnife systems. Error bars indicate the estimated range of measured values due to a change in field diameter by ±0.2 mm.

Iris field size repeatability of 0.2 mm. The 0.2 mm uncertainty translates into an output difference of up to 10%, 3%, and 1.4% between individual Iris beams of 5 mm, 7.5 and 10 mm diameter respectively (Figure 3). To reduce the clinical impact, the manufacturer has implemented restrictions for using the 5 mm Iris aperture: Solo delivery of 5 mm beams is prohibited and the MU contribution of 5 mm beams within a plan is limited to allow for a maximum expected error of 2% to the prescription dose. This MU tolerance is hard coded within the planning software based on the assumption of 15% output variation in 5 mm Iris beams.

This variation in output factors supports the recommendation that the Iris field size be verified after field size calibrations and during monthly QA to a size within 0.2 mm of the field sizes found at the time of the original Iris beam commissioning. It is important to understand that accepting a larger than 0.2 mm difference in field size translates into covering a volume with the prescription isodose that may be smaller or larger by the same amount, and that absolute dose for the smallest fields may deviate by several percent (e.g., ±3% for the 7.5 mm field) due to changes in the output factor. This degree of uncertainty can be clinically unacceptable, arguing for the use of QA methods capable of detecting field size changes as small as 0.2 mm, or to deliberately limit the use of small Iris field sizes beyond the restrictions put in place by the manufacturer.

2.5.2 | Methods for Iris field size verification

Since the Iris was introduced, several methods for field size verification have been and are still being developed. A selection of established methods is described

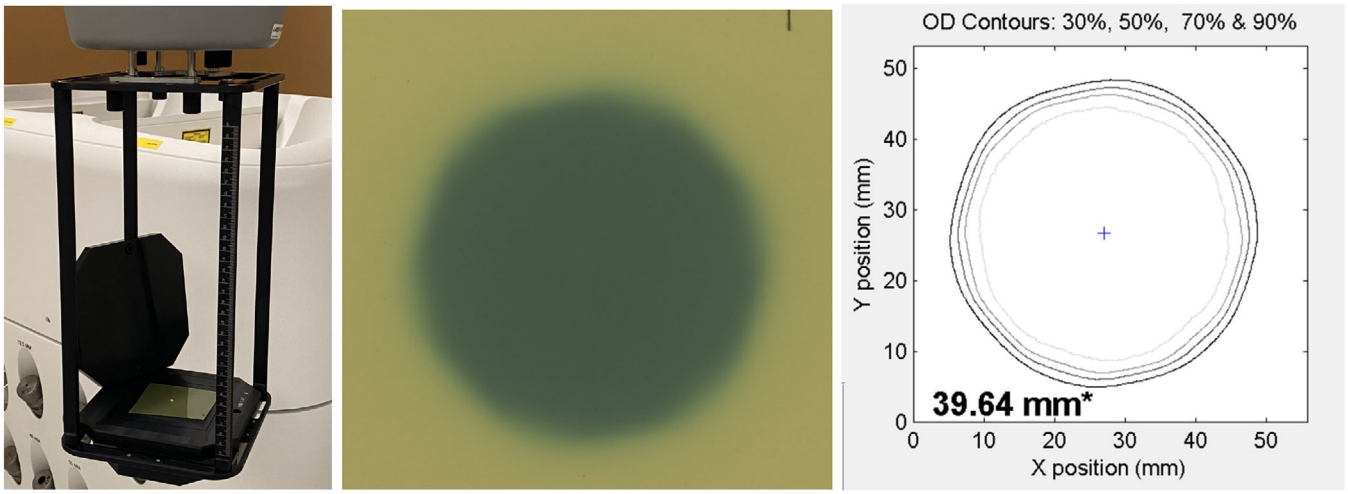

FIGURE 4 Birdcage with film holder for IQA (a), an example radiochromic film image of a 40 mm Iris field (b) and its optical density contours (c). The alternating two penumbra sizes can be seen around the field periphery.

below, emphasizing time expenditure and accuracy of the procedure.

Gafchromic film (EBT2, EBT3) measurements

This is the standard method supported by Accuray as part of the complement of QA tools provided with the purchase of a CyberKnife system ("Iris QA—IQA"). It consists of Acrylonitrile Butadiene Styrene (ABS) blocks that attach to the distal end of the "bird-cage" assembly (Figure 4), providing a fixed radiation buildup and backscatter layer for the exposure of radiochromic films and a software tool for film analysis. Baseline data from films exposed to Iris fields at the time of commissioning are used as the comparison standard.

Advantages are that a sampling of field sizes can be quickly measured and the actual radiation field is the source of sizing information. Disadvantages are that establishing a baseline measurement set with multiple measurements is time consuming and that the accuracy of the IQA method is very dependent on a careful, reproducible management of the film exposure and scanning process. Absolute accuracy and reproducibility of the IQA method smaller than 0.5 mm has been demonstrated,[12] but is difficult to reliably achieve. Due to the lack of published data on this technique, this TG concludes that the overall accuracy is 0.5 mm. Reproducibility of IQA results can be expected to be better for newer Iris versions due to improved field size repeatability, but there is no published data yet.

Direct image-based measurement

This method images the Iris segments directly using a video or digital camera with fixed optics in a rigid, reproducible geometry. Images of the segment positions are captured and analyzed manually or by automated software, which allows for very quick field size measurements. A disadvantage is that radiation is not used. Collimating segment position is measured directly and can be compared to a baseline but differs from the radiation beam size produced in a medium.

TABLE 2 Overview of Iris field size verification methods and characteristics.

Method	Time (h) (12 field sizes)	Accuracy (mm)
Film (IQA)	2.00	±0.5
Direct image	0.50	±0.2
Dose area product	0.50	±0.2
Radiation imaging devices	0.25	±0.2

Accuracy is claimed by the manufacturer to be in the 0.1–0.15 mm range, which is in agreement with a report on performance of a prototype[13] and the statistical errors (indicating reproducibility of measurements <0.2 mm) shown in Table 2. The dimension measured is the actual segment aperture size which is approximately half the field size at the reference distance of 80 cm. There is no commercially available product for this method currently.

Dose area product/Bragg peak parallel plate ionization chamber measurements

This method uses a parallel plate ionization chamber large enough to encompass the full radiation field cross section of the largest Iris field size at the distance the chamber is mounted. Comparisons are made for all Iris field size settings and one, or preferably more, standard fixed field collimators. The parallel plate ionization chamber produces a partial volume ionization current reading where the magnitude is proportional to the product of the fraction of the covered chamber volume and

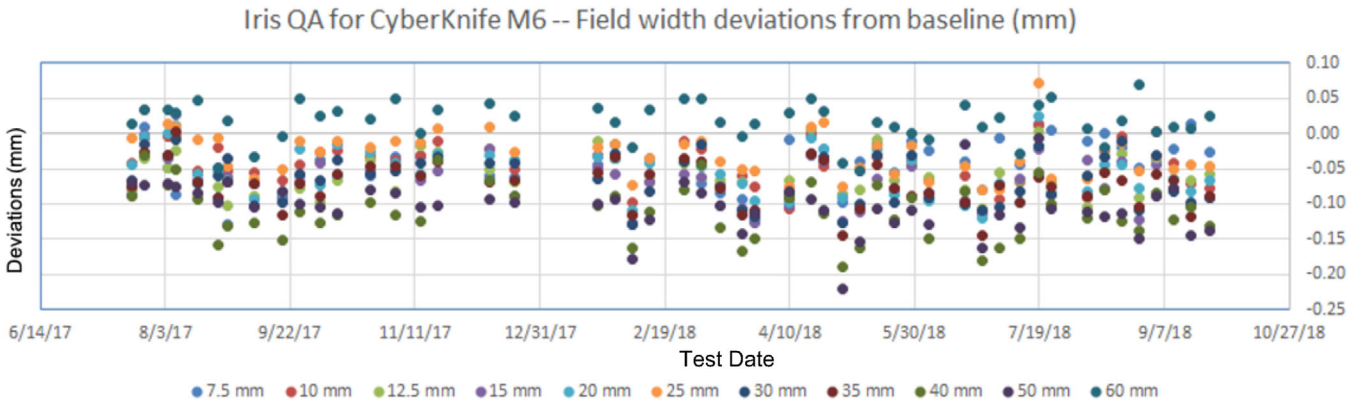

FIGURE 5 Iris QA results (Stanford University) from a StereoChecker (Standard Imaging Inc.). The results are compared with one set of baseline measurements taken in April 2017. Standard deviations on the QA data for all 11 collimators are between 0.03 and 0.04 mm.

the OF. The ratio of Iris partial volume ionization readings to the fixed collimator readings is the measurement parameter. The advantages are a good discrimination of small changes in field size especially for the smallest field sizes, the method uses the actual radiation beam, and that measurements for all field sizes can be made quickly using a single, simple instrument setup. The disadvantages are that this method is a secondary comparison, not an actual field size measurement, which does not allow for visual inspection of the field shape, and changes in the primary beam can impact results, which can be overcome to some extent by using multiple fixed cones as reference. Temperature and pressure should be monitored over the course of measurement as well. By deliberately introducing small changes in the Iris field size, it can be demonstrated that deviations of 0.2 mm can be reliably differentiated for the largest cones, with smaller deviations differentiated for smaller fields.[14,15]

Iris QA using radiation imaging devices

A commercially available portable electronic portal imaging device (EPID), StereoChecker (Standard Imaging Inc.), is currently available for Iris QA. This device includes embedded fiducials to facilitate alignment of the detector using the stereoscopic kV system. In this method the imaging device is exposed to one anterior beam at all available Iris apertures, and the field sizes are measured and compared to baseline data acquired at the time of Iris commissioning.

The advantages are that field sizes can be measured very quickly, and the actual radiation field is the source of sizing information. The disadvantages are the weight and cost of the device. Accuracy is claimed to be 0.1 mm by the manufacturer. Considering the repeatability specification of the Iris aperture, it can be expected that deviations of $\leq$0.2 mm can be identified with one set of measurements, which is in agreement with reported maximum deviations of $<$0.2 mm in measurements over 8 months (Figure 5).[16] Iris QA using a radioluminescence-based imaging phantom has recently been reported. This could be an in-expensive alternative.[17]

Summary of Iris field size QA

Published long-term data on stability of the Iris subsystem is sparse. Three groups consistently reported stable Iris field sizes over the course of 2 years in monthly QA measurements.[12,14,15] One of the groups reported that field size consistency of $\pm$0.2 mm can be maintained for a current Iris v3, when appropriate QA methods are employed.[15]

On this basis, this task group recommends a monthly frequency for Iris field size QA, but acknowledges that additional long-term data would be valuable. A tolerance level of $\pm$0.2 mm for field size changes is preferred. Minimal acceptable tolerance level is $\pm$0.5 mm for field sizes (FS) 10 mm and above which is in agreement with MPPG 9a recommendation. In the latter situation we recommend deliberately limiting the use of small Iris field sizes beyond the restrictions put in place by the manufacturer.

2.6 | Iris commissioning and QA recommendations

In analogy to fixed cones, OCRs, TPRs, and OFs have to be measured during commissioning. The commissioning procedure and measurement setup are explained in detail in the manuals provided by the vendor.[11] To incorporate the dodecagon shape of the Iris in OCRs, four sets of profiles (short: 0°, 90°; long: 15°, 105°) are measured and averaged. Accurate alignment of the water tank motion axes is critical to correctly record short and long profiles. To minimize the impact of Iris field size repeatability which is particularly important for the two smallest field sizes (5 mm and 7.5 mm), OFs should be determined by averaging multiple measurements, with Iris being resized between repeated acquisitions. AQA and E2E should be performed and baselines

TABLE 3 Summary of QA recommendations for the Iris collimator.

Parameter	Frequency	Tolerance	Method
Iris beam CAX / Laser coincidence	Quarterly / Commissioning / Path Calibration	Preferred: <0.5 mm Acceptable: <1.0 mm	Film, water tank
Beam QA (OCR, TPR/PDD, OF and FWHM) (Section 7.3)	Commissioning, annual	Consistent with commissioning (Table 10)	Water tank
Field size consistency	Monthly/Recalibration	Preferred: ±0.2 mm from baseline Acceptable: ±0.5 for FS ≥ 10 mm	Film, camera, dose area product, EPID
End to end targeting	Commissioning/Annual/Monthly	Static E2E: <0.95 mm Synchrony E2E: <0.95 mm preferred, <1.5 mm acceptable	Film
AQA targeting	Daily	<0.95 mm from baseline	Film
DQA (Section 3.5.4 and 7.2)	Commissioning/Monthly	2%/2 mm (>90%) for static and 3%/3 mm (>90%) for motion tracking	Depends on equipment availability

established for daily, monthly, and annual QA. DQA should be performed before the system is ready for clinical use and periodically after as recommended in the original TG 135 Report.[1] More discussion on DQA is given in Sections 3.5.4 and 7.2. A subset of the commissioning data should be checked annually.[1] A summary of annual QA and tolerances are given in Section 7.3. The QA recommendations for Iris are summarized in Table 3.

3 | InCise MLC

3.1 | Introduction

The CyberKnife MLC was introduced as an optional collimator system available on the CyberKnife model M6 and S7 with the intent for more efficient dose delivery. The first model, InCise, was released in 2014,[3] followed by an updated model, InCise 2, in 2015.[4] The two MLC versions are different in MLC leaf width and maximum open field size but have similar mechanical design and physical characteristics. The description in this chapter is focused on the second version, but the recommendations are applicable to both versions, unless stated otherwise.

The MLC can produce a 10 × 10 cm^2 field that could be employed for reference dosimetry. However, the manufacturer has designed the software such that the 6 cm fixed cone remains the only CK reference field because the MLC is optional hardware for the CyberKnife M6/S7 and is not available on all previous models. Plans using MLC were reported to have significant reductions in MU and treatment time with a better dose drop off in the low dose regions.[18–20] The MLC allows one continuous opening in one segment. Any segment opening must be at least two leaf widths wide. The individual leaf opening must be larger than 5 mm, and with a minimum open area of 57.75 mm^2. Considering a relative inferior beam penumbra and minimum opening limitation, very small targets (size <7.5 mm) may not be candidates for MLC based planning.[18]

3.2 | Mechanical description

The InCise collimator system is composed of two banks (X1 and X2) of Tungsten MLC leaves weighing approximately 50 kg in total (Figure 6a). The initial version, InCise MLC, was designed to achieve a maximum open field of 120 × 102.5 mm^2 using 41 leaf pairs of width 2.5 mm each at 80 cm SAD. The second version, InCise 2 MLC, was designed with a maximum open field of 115 × 100.1 mm^2 using 26 leaf pairs of width 3.85 mm at 80 cm SAD. The leaves are 90 mm high and the leaf ends are defined by three surfaces focused on fully retracted, mid-travel and fully over-traveled positions (Figure 6b) at 80 cm SAD. The lower end of the leaf is 40 cm away from the source, the same as the fixed cone and Iris collimators, which ensures similar clearance during delivery. The leaves are tapered to focus on the radiation source in the direction perpendicular to leaf travel. Unlike other MLCs with tongue and groove design to reduce inter leaf leakage, the InCise MLC has flat side surfaces which allow full interdigitation (The leaves from two banks can cross each other.) and full leaf over-travel (The leaves from one side can fully travel to the other side to close the field). To minimize the interleaf leakage, the whole leaf set is tilted 0.5° about the IEC *X* axis (i.e., the leaf travel direction). The manufacturer's specification on maximum interleaf leakage is <0.5%.[11] Similar to fixed cone and Iris collimators, the MLC assembly is mechanically aligned with the beam central axis through the tool plate attachment (Figure 6a). Coincidence checks between the field laser,

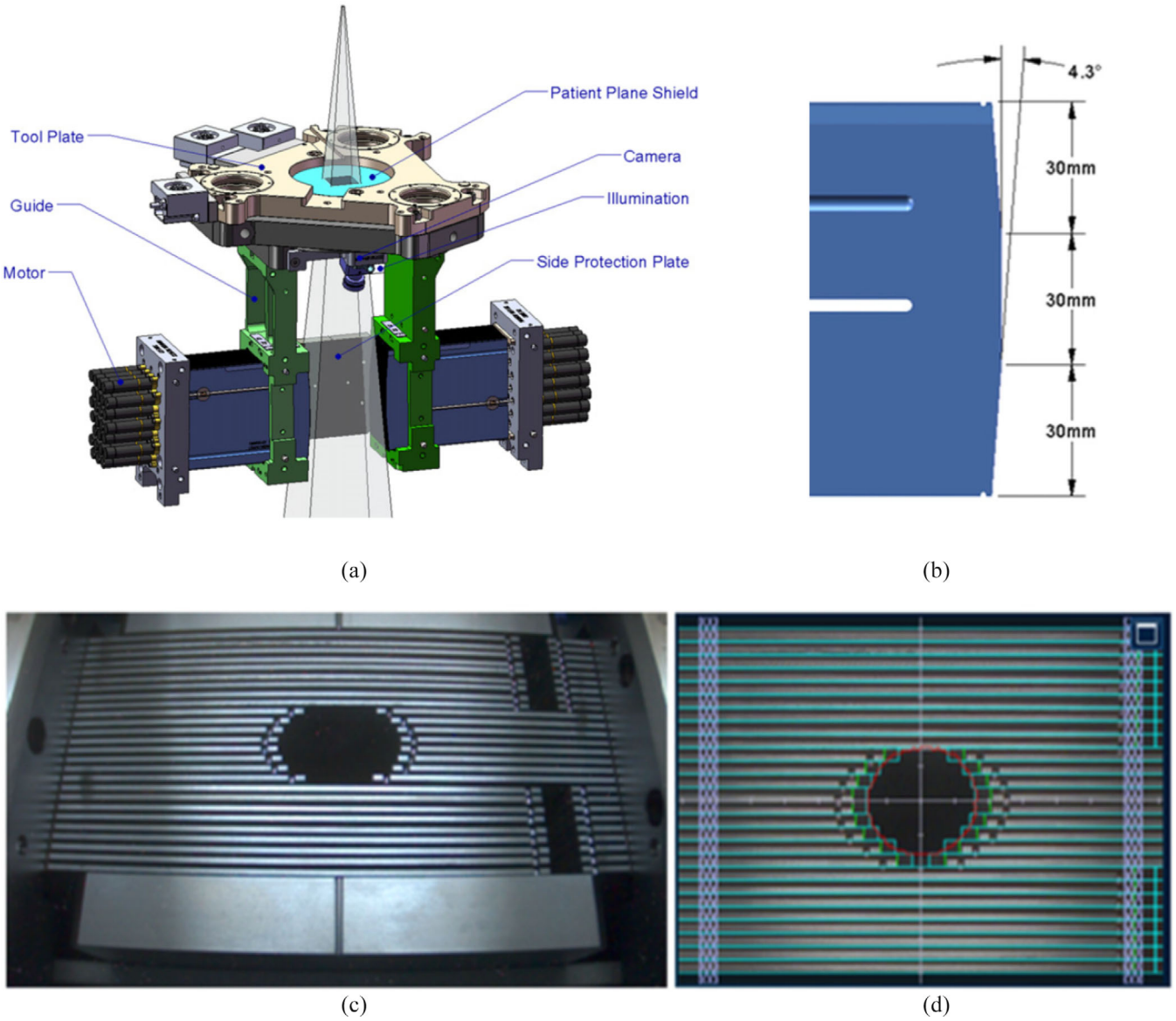

FIGURE 6 This figure displays the mechanical design of the second version, InCise 2, MLC: (a) illustration of the mechanical structure of the InCise 2 MLC, (b) three-edged leaf end design, (c) an original video image from the secondary feedback camera, (d) the corrected secondary feedback image displayed with planned MLC and plan target overlaid.

center of the MLC field, and the center of the other collimators should all be within 1.0 mm at 80 cm SAD. Collimator exchange is automated with robotic operation as described in the previous section for the Iris collimator.

3.3 | MLC calibration and leaf end correction

The MLC leaves can move independently to each other with each leaf driven by a brushed DC motor with a maximum leaf speed of 25 mm/s (at 80 cm SAD). Each motor has an encoder used to track the incremental motion of the leaf at a resolution of ±50 μm (at 80 cm SAD). Since the motor encoders only track relative movement, a positioning calibration needs to be established during the installation or after adjustments during field service. The leaf position calibration is achieved with four mechanically stable optical beams positioned at the rear and front of the leaves perpendicular to the leaf travel, two for each leaf bank. Each optical beam impinges on a photo diode detector. The optical beams serve as mechanical stable reference positions for the MLC. The calibration process sets the zero positions of the motor encoders and establishes the baselines for the initialization process. More detailed information on leaf calibration can be found in the published literature.[4] As described above, the leaf banks are calibrated separately, thus are prone to residual offset between the

banks possibly causing the actual field sizes to deviate from nominal. These residual errors are removed by applying a global correction offset on each bank. The correction offsets are detected on multiple garden fence tests (see Section 3.5.3) during installation.

The initialization process is initiated by the delivery software before each fraction of treatment as a security check.[4] This process repeats the calibration process. An interlock turns on when the detected encoder values exceed the baselines (above ±0.2 mm). The initialization process protects against optical beam shifts and other mechanical anomalies or changes from the time of system calibration.

Because of the non-focused three-edged leaf end design, the radiation partial transmission introduces offsets between the radiation edges and the leaf mechanical edges. The offsets are directly related to the leaf end design and photon beam energy and are not uniform throughout the leaf travel. They are minimized at the wide open, central axis (CAX), and fully over-traveled positions; and are maximized at the positions halfway from the CAX. Correction offsets are applied in addition to the calibration within the delivery system to remove the leaf end effects on the field sizes.[4] The correction offsets are obtained by modeling the leaf tip transmission as a function of leaf position using a simple ray-trace attenuation calculation, ignoring the scattered radiation. No extra measurements of the radiation leaf end offsets are required during MLC installation and commissioning.

3.4 | Secondary MLC position verification system

The camera based secondary MLC position verification system is only implemented with the second version of the MLC (the InCise 2 MLC). This system provides a secondary mechanism of detecting MLC leaf positions with accuracy of better than ±1.0 mm.[4] The camera (Computar Optics Group, Cary, NC, USA) is located obliquely above the MLC leaf banks (Figure 6a). The oblique image is first corrected, and then used for position detection via the leaf end features, such as the notch near the leaf tip (Figure 6b). The system is capable of tracking individual leaf positions with approximately a 4 Hz update rate. The position verification is performed immediately before and after the delivery of every MLC aperture, but not during the beam on time. Upon failure of verification (difference >1 mm according to manufacturer's specification), a system interlock occurs. Figure 6c shows the original detected image. The system only displays the processed image with optional graphic overlays of leaf positions as specified in the treatment plan and as measured by the primary and secondary feedback systems (Figure 6d). This feedback system is independent of the MLC primary control system; therefore, the video stream can be used as a visual examination and is an extra security check of the treatment. Currently no QA method is provided by the vendor for this secondary MLC position verification system.

3.5 | MLC physical characteristics and QA

3.5.1 | Path calibration and targeting accuracy

CyberKnife dose delivery with MLC employs a step and shoot delivery method. Multiple segments generated from inverse planning are delivered at the predesigned node positions to achieve an intensity modulated radiation distribution. The MLC body and head paths, which are composed of the set of the predefined delivery nodes in body and head treatments, are independent from those of the circular collimators. To accommodate the slightly bigger MLC housing, the MLC body and head paths contain a slightly lower number of nodes (102 and 171 nodes in the MLC body and head paths respectively) than those in the circular collimator body and head paths (117 and 179 nodes in fixed/Iris body and head paths respectively). A separate path calibration (explained in the previous TG 135[1]) followed by a separate Deltaman correction (a software based systematic error correction[1,11]) is required during commissioning. The geometric path calibration accuracy relies heavily on the coincidence between the MLC field center and the field laser. QA on the MLC field center and field laser coincidence, as well as the robot targeting QA follows the same recommendations as for fixed and Iris collimators.[1,11] The field center and laser coincidence should be checked quarterly and agree to within 1.0 mm at a distance of 80 cm from the radiation source.[1] For the robot targeting check, independent E2E tests using the MLC should be performed for all the available tracking modes during the commissioning and be selectively tested monthly in alternation with fixed cones and Iris. An MLC based AQA baseline should also be established during the commissioning and be performed in daily rotation with fixed cones and Iris. Concepts of AQA and E2E tests using MLC are similar to that for fixed cones, which are well described in the PEG.[11]

3.5.2 | Leaf transmission and penumbra

The InCise MLC is designed to have a maximum leaf transmission <0.5%. This is accomplished by tilting the whole MLC assembly by 0.5° away from the source to minimize the interleaf leakage. The average leaf transmission is reported to range from 0.22% to 0.25%,[4] which is higher than that of the CyberKnife fixed cone (<0.12%) and Iris collimators (0.05%).[2,4] To eliminate

interleaf end leakage the MLC leaf ends are always positioned under the primary collimator when they are not used for the segment opening. The leaf transmission measurement is usually conducted with film; the detailed measurement procedure is described in the PEG.[11] This task group recommends leakage measurements should be performed for both leaf banks with film during commissioning and annually. The maximum leaf transmission should be <0.5%.

The direct impact of the tilting of the MLC assembly is the non-symmetric penumbra in the direction perpendicular to leaf travel (IEC *Y* axis). The Y2 penumbra is found to be 0.5 mm larger than the Y1 penumbra on average.[4] Due to the three-edged leaf end design, field penumbra is expected to be slightly larger than that of the fixed cone which has a double focused design. The treatment planning system uses the finite size pencil beam algorithm (FSPB) and Monte Carlo algorithm for MLC dose calculation. The penumbra difference in the *Y* direction is ignored in the FSPB calculation and is included in the Monte Carlo calculation. Based on the committee's experience so far, ignoring the penumbra difference in the FSPB calculation does not introduce a significant impact on dosimetry.

3.5.3 | Leaf position QA

Leaf position accuracy is a crucial component in step and shoot delivery. Leaf position QA is done using the vendor recommended garden fence tests,[11] developed by Bayouth et al.[21] This test is performed using a manufacturer designed special phantom as shown in Figure 7a,b. The phantom is designed to be tightly attached under the MLC and mechanically aligned with the radiation field. There are two Tungsten pins mechanically secured to coincide with the center of the field and with the *Y* axis. The buildup piece is 1.5-cm-thick solid water, and the film to target distance is 433.5 mm. The garden fence test delivers strips of open fields over the maximum range of the open field size. Figure 7c shows a five-strip test (10 mm wide strips with 15 mm gap) aligned using the two markers with the MLC template overlaid. The detected leaf edges were compared to the planned leaf positions for position accuracy. The advantages of this design are easy alignment and flexibility in delivery angles. The task group recommends that the tests be performed at head vertical position (leaf travel horizontal) and head horizontal position (leaf travel vertical with maximum gravity impact, X1 on top or X2 on top). The manufacturer's recommendations should be followed for leaf accuracy: more than 90% of the tested positions agree <0.5 mm, all tested positions agree <0.95 mm, and the average deviations are <0.2 mm. For evaluation, the detected deviations at 433.5 mm should be converted to their values at 800 mm distance by multiplying by 1.85.

The MLC performance has been verified by multiple groups to be within the vendor's specification. Asmerom et al.[4] investigated the impact of MLC position reproducibility on the output factors of the smallest deliverable field (7.6 mm x 7.7 mm). Ten output measurements with repositioned MLC leaves agreed within 0.1%.[4] The gravity impact on leaf position was reported to be 0.1 mm for the InCise 2 MLC,[4] and 0.2 mm for the first version MLC.[3] Long-term failure mode analysis is not currently available for the CyberKnife MLC. Two years of monthly QA measurements of mean position deviations (corrected to 80 cm SAD) are presented in Figure 8. The error bar represents one standard deviation. Two measurements at MLC vertical position and MLC horizontal position were performed each month. The results are all within manufacturer recommended tolerances. No significant gravity impact on leaf positions was observed. The measurements were conducted with EBT3 films. A typical test result is shown in Figure 7d. The tolerance was set to ±0.27 mm to account for the 433.5 mm source to film distance.

The above film-based garden fence test is time consuming. For daily QA, a standard picket fence test, 10 strip fields abutting each other, is recommended for visual examination.[22,23] This film based daily QA procedure is well described in the manufacturer's PEG.[11]

3.5.4 | DQA and patient QA

The previous TG 135[1] recommended non-isocentric patient QA (DQA) for CyberKnife be done for the first several patients for every tracking modality after commissioning, and quarterly afterwards. This decision was based on the fact that all 12 fields for fixed and Iris collimators were fully characterized and validated during commissioning.[1] This justification does not apply to plans generated using the MLC, which are similar to plans generated by MLC systems mounted on C-arm linacs. Therefore, patient specific QA recommendations for MLC-based CyberKnife delivery should follow published reports on SBRT.[25–27]

While current recommendations require measurement-based IMRT QA for every patient, there are ongoing efforts questioning the need for it. Recent data analysis on the effectiveness of QA tests[28–31] provided evidence that traditional DQA is not sensitive to minor planning errors, but effective in identifying rare catastrophic failures. Tools such as EPID in-vivo dosimetry,[29] which has been shown to be highly effective in detecting errors on C-arm linacs, are not available on the CyberKnife. A recent study also showed that independent recalculation outperformed traditional measurement-based IMRT QA methods in detecting unacceptable plans.[31] We understand that this study is based on C-arm linac IMRT delivery, but the result should be applicable to CyberKnife under the condition

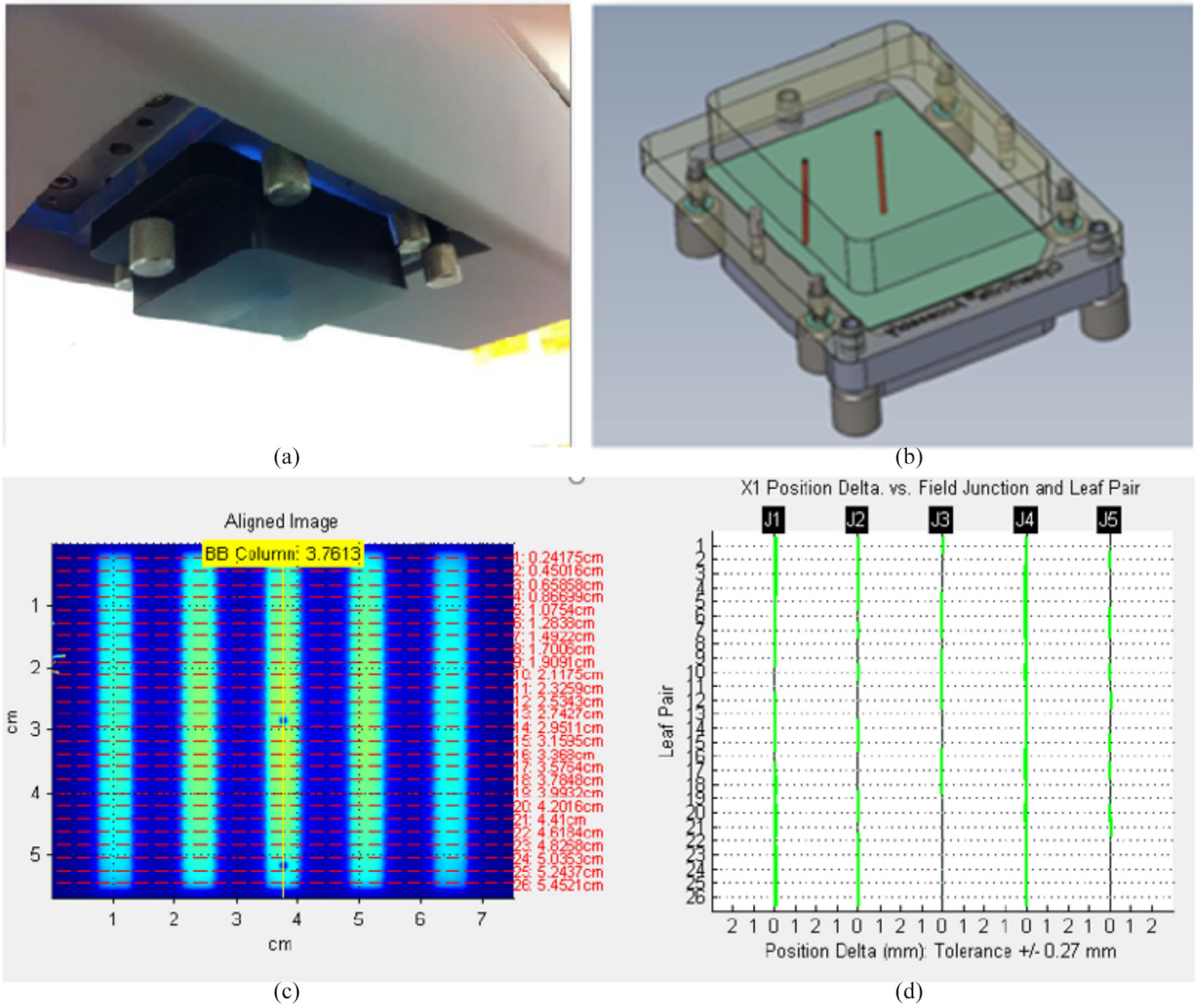

FIGURE 7 (a) The MLC QA phantom is directly attached under the MLC. (b) The QA phantom with two Tungsten pins defining the center of the field and the *Y* axis. (c) The dose pattern of the garden fence film with the Tungsten markers identified and MLC template overlaid. (d) Analyzed results with tolerance of ±0.27 mm at 433.5 mm SAD.

that the QA on targeting accuracy is strictly performed on a daily basis and a 3D 2nd check calculation system with comparable accuracy is available.[32]

For safety reason, the CyberKnife MLC performs a thorough accuracy test of each MLC leaf through initialization every time before a plan delivery (Section 3.3). Additionally, the CyberKnife InCise 2 MLC is equipped with an independent camera-based monitoring system which is capable of monitoring the MLC position in <1 mm resolution, as stated by the vendor. The current MLC camera is only monitoring between leaf segments and QA methods for the device do not exist at this time. One proposed method to reduce the patient-specific QA measurement for CyberKnife MLC cases is to utilize a camera-based MLC monitoring system in combination with an independent 3D dose calculation verification system.[32] Monte Carlo based independent 3D dose calculations are now available in multiple commercial software systems. The recent published TG 218 report[33] on tolerances and methodologies for gantry based IMRT QA provides useful information for patient QA measurements, however it may not be fully applicable to CyberKnife, which involves additional degrees of freedom due to its non-isocentric delivery format, and lack of an on-board detector system such as EPID. A similar publication on CyberKnife patient-specific QA is not currently available.

Due to the image guided delivery and the involvement of numerous non-coplanar, non-isocentric small beams, CyberKnife patient-specific QA is time consuming and technically challenging. Traditional methods have mostly relied on ion chambers and film.[34]

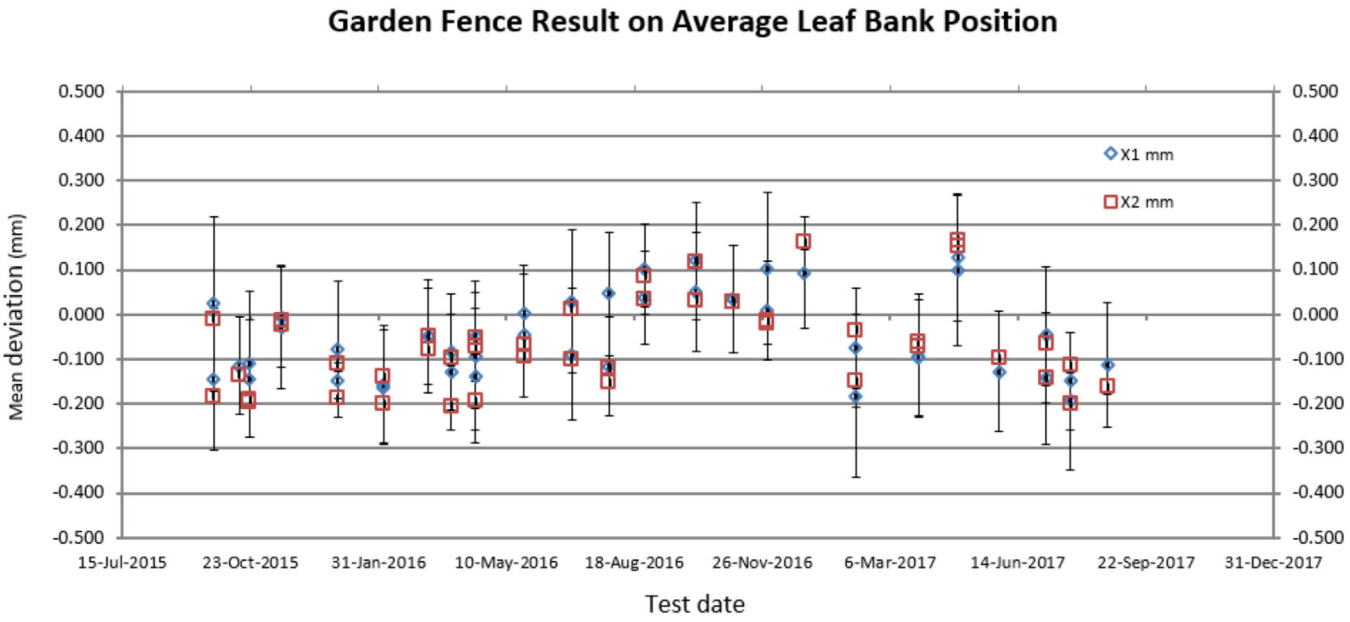

FIGURE 8 Two years of monthly QA for an InCise 2 MLC using the film garden fence test (Stanford University) is shown. Mean deviations for the two leaf banks are displayed. Two tests were performed each month, one at head vertical position and one at head horizontal position with MLC travel vertical, either X1 on top or X2 on top.

Patient-specific QA using commercially available 2D detector arrays have become available.[35–38] 2D detector arrays are convenient to use, providing nearly instant results. Spatial resolution has been significantly improved on most recently reported solid state detector arrays,[37–39] making them suitable for very small targets. Angular or dose rate related corrections may need to be considered if they are not included in the vendor provided data analysis software.[33,36,39] Although QA time with detector arrays is significantly reduced compared to film-based QA, it can still be very long (15–30 min just for plan delivery) due to the robot transit times between many delivery nodes. Perpendicular field-by-field and composite delivery is less time-consuming, however it does not reflect the characteristics of a non-isocentric, non-coplanar treatment machine.

Considering that the MLC system is still relatively new and should be carefully vetted in diverse clinical situations, this task group recommends performing patient-specific QA until further data on plan robustness and failure modes becomes available. Minimally we also think monthly DQA is acceptable provided the institution is well experienced; a good systematic routine QA is established; and an independent secondary 3D dose calculation is implemented as a complement verification method.[32] Dosimetric verification techniques should include measuring two-dimensional dose distributions. Measuring a point dose only, while providing valuable information, is not considered sufficient to constitute a full delivery quality assurance. TG 135 tolerances on DQA[1], 2%/2 mm (>90%) for static and 3%/3 mm (>90%) for measurements with motion tracking, should be adhered to for MLC based patient QA to maintain a consistent standard.

The above TG 135 tolerances provide a general guidance on CyberKnife patient QA. However, we acknowledge that the tolerances could be dependent on the QA methods and treatment sites (target sizes). We agree with TG 218[33] recommendations that each institution should analyze their QA statistic data and develop their own tolerances based on their own QA equipment and clinical setting.

3.6 | MLC commissioning and summary of QA recommendations

Beam data (OCRs, TPRs, and OFs) is required to be measured at various field sizes and depths in a water tank system for MLC commissioning. The commissioning procedure and measurement setup are explained in detail in the manuals provided by the vendor.[11] Robot targeting QA (AQA and E2E) should be performed and baselines set up for daily, monthly, and annual QA.[1,11] DQA should be performed before the system is ready for clinical use.[1] DQA and patient QA are discussed in Section 3.5.4. A subset of the commissioning data should be checked annually as recommended in the previous TG 135.[1] Beam QA tolerances are updated in Section 7.3 (Table 10).

The QA recommendations for the CyberKnife MLC are summarized in Table 4 For additional general MLC QA information, the AAPM TG 135.B recommends referring to AAPM TG 50,[22] AAPM TG 142,[23] and AAPM MPPG 8.a/MPPG 8.b.[40,41]

TABLE 4 Summary of QA recommendations for the MLC collimator.

Parameter	Frequency	Tolerance	Method
MLC beam CAX / Laser coincidence	Quarterly/Commissioning / Path Calibration	Preferred: <0.5 mm Acceptable: <1.0 mm	Film, water tank
Beam QA (OCR, TPR/PDD and OF) (Section 7.3)	Commissioning /Annual	Consistent with commissioning (Table 10)	Water tank
MLC position quantitative test	Commissioning/Recalibration/ Monthly	>90% deviations <0.5 mm, mean deviation <0.2 mm, all <0.95 mm	Garden fence test with film
MLC position visual examination	Daily	NA	Picket fence with film
MLC leakage	Commissioning/Annual	Max transmission <0.5%	Film
End to End targeting	Commissioning/Annual/ Monthly	Static E2E: <0.95 mm Synchrony E2E: <0.95 mm preferred, <1.5 mm acceptable	Film
AQA targeting	Daily	<0.95 mm	Film
DQA/Patient-specific QA	Commissioning/Preferred: Per plan Acceptable: monthly	2% /2 mm (>90%) for static and 3% /3 mm (>90%) for motion tracking	To be decided by user based on availability

4 | MOTION TRACKING QA

4.1 | Introduction

For treatment of moving targets, CyberKnife uses the Synchrony motion tracking system that tracks the tumor actively. A major component of the Synchrony system is a flashpoint camera mounted on an adjustable arm attached to the ceiling near the foot end of the patient couch. This camera monitors three tracking marker LEDs attached to the patient chest for external skin motion and an algorithm correlates the external skin movement to the internal tumor positions detected by the orthogonal kV x-ray imagers. A correlation model is first established between the external skin movement and internal tumor positions at eight breathing phases before treatment and is used to predict the tumor position during the treatment (Figure 9a,b). The basic technical concepts of Synchrony tracking have been described in several publications.[42–45]

While the basic Synchrony concepts remain the same, substantial changes were introduced to Synchrony motion management since the publication of the previous TG 135 report.[1] The newer version extended Synchrony treatment to Xsight Spine tracking (only Fiducial and Xsight Lung tracking were available in earlier versions) with the patient in the prone position (Xsight Spine prone). Xsight Spine prone mode was designed to allow posterior beams for spine treatment, however the benefit was reported to be insignificant if an extra margin is required to compensate for target motion.[46] The newer versions also introduced Lung Optimized Treatment (LOT) allowing 1-view or 0-view fiducial-less tracking for lung treatment (Section 5). In addition, various improvements in model generation and visualization were implemented. For brevity of this report, this section focuses on aspects of the Synchrony model-based real-time tracking which has direct impact on QA or clinical code of practice.

4.2 | Placement of the optical markers

The skin motion is monitored by the Synchrony camera at a frequency of 30 Hz through three tracking marker LEDs attached to the patient's chest. For better signal to noise ratio on skin traces, the LED skin markers should be placed near the position of maximum body motion due to respiration, which should be identified during patient treatment setup. However, for Xsight Spine prone patients, the tracking markers are recommended to be placed as close as possible near the target location while maintaining an acceptable signal to noise ratio. Since the skin near the target location should better correlate with the target, this placement potentially minimizes errors introduced by an imperfect correlation model. The position of the Synchrony camera should be directly in line with the LED tracking markers.

4.3 | Generating and updating the correlation model

A correlation model maps the tumor position (*X*, *Y*, *Z*) in the patient coordinate system (detected by the in-room x-ray system) with the markers' movement R. The maximum movement direction in the camera coordinates (Xc, Yc, Zc) is used as R (Figure 9a). Since the chest movement is mostly in the anterior-posterior direction, the Yc signal will likely be chosen as R. During Synchrony tracking, the CyberKnife system uses the correlation model to predict the tumor position (*X*, *Y*,

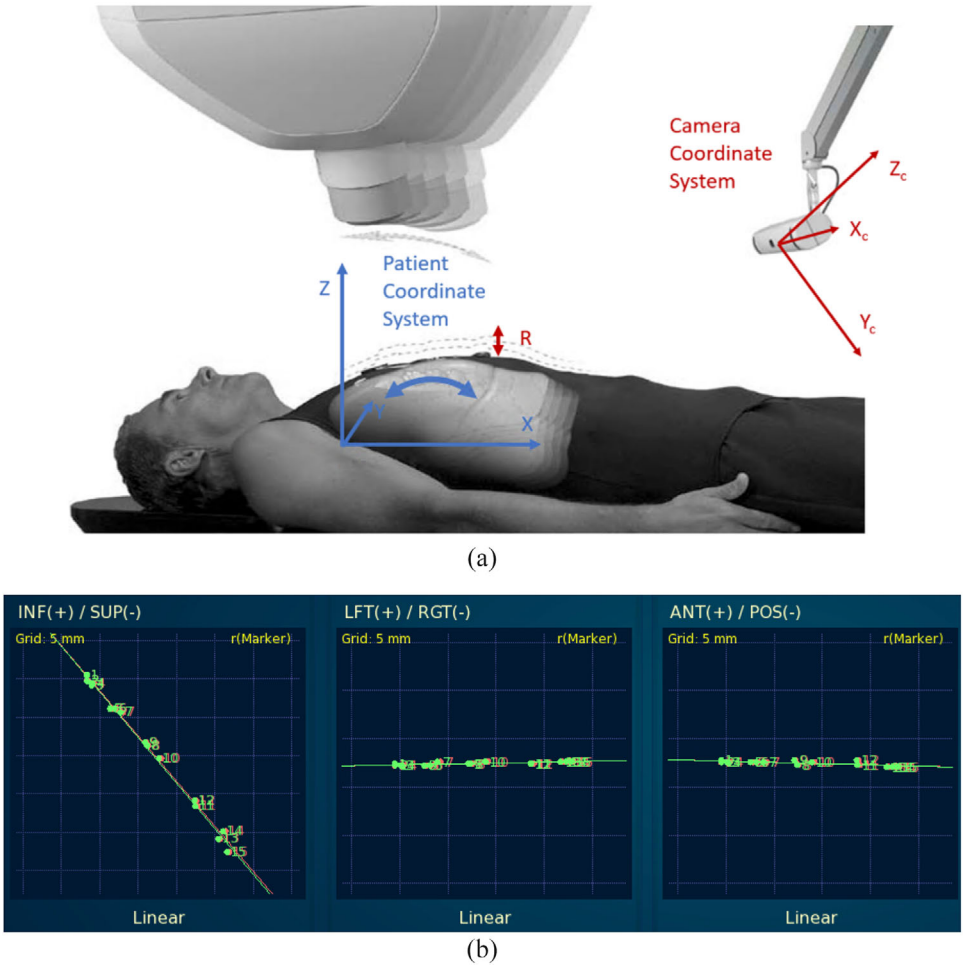

FIGURE 9 An illustration of Synchrony treatment: (a) the skin movement R detected by the Synchrony camera in camera coordinates is used to predict the tumor position (*X*, *Y*, *Z*) in the patient. (b) A correlation model (linear model displayed) is established between the tumor location (*X*, *Y*, *Z*) and marker movement R.

Z) 115 ms in the future for robot correction. One hundred fifteen millisecond is the systematic time delay in relaying the present tumor position and adjusting the robot coordinates to dynamically deliver the dose. Three model types, linear, curved and dual poly, are available[11] and the model type that fits the best for treatment (minimize standard deviation on 15 fitting points) is automatically employed by the system. With the correlation model, the system is able to continuously track the tumor, while delivering the dose with 100% duty cycle.

Model generation, with the automated modeling option and fast imaging (burst imaging mode), is significantly improved from previous versions of the software. During model generation, one point is added to the synchrony correlation model each time a live x-ray image is acquired. To obtain an accurate model, the model points should be distributed evenly and cover the whole range of respiratory motion. The synchrony system categorizes the correlation model as optimal if at least seven of the eight phases (the whole breathing cycle is split into eight phases) of the respiratory cycle are included in the model, including points for full inspiration ("peak") and full expiration ("valley").[11] The Synchrony system actively controls the timing of image acquisitions to cover all phases of the breathing cycle.

While a valid synchrony model could be built with a minimum of three model points in earlier versions or four (peak, valley, in-/expiration midpoints) model points in the newer version, additional model points are recommended for better model accuracy. During treatment, up to 15 model points are stored and are updated using the "First-in First-out approach."[47] Any unexpected movement (with default tolerance of 5 mm) of the Synchrony camera, LEDs, and/or the patient will invalidate the Synchrony model and require a model re-generation before resuming the treatment.

In the newer software version, a "burst mode" is implemented which allows for rapid acquisitions of multiple images at 1 s intervals. During model generation, a burst is employed to quickly fill the model with 15 points. During delivery, the model is updated in bursts of three

images (replacing the three oldest model points) instead of one image at a time. While this feature speeds up treatment and enables faster model generation and updates, imaging intervals during treatment automation must be extended to avoid excessive x-ray exposure. At each burst, the user is required to visually verify lock-on results of three image pairs at a time, which can be challenging for LOT (discussed in Section 5). For cases with inconsistent lock-on, the burst mode should be disabled.

4.4 | Rotational correction

The robotic delivery is capable of 6D corrections (three translational and three rotational). However, in some cases, it is not possible to correct for target rotations. This happens for LOT tracking and when insufficient fiducials are identified at the delivery console. In addition, when fiducials are used for tracking, the rotation detected from the fiducials may be significantly different from the rotation based on the patient's bony anatomy due to the tumor rotation within a respiratory cycle or tumor deformation. In that situation, assessment through visual examination or kV imaging on spine alignment is recommended and rotational corrections may be turned off.

If rotations cannot be determined with the treatment plan or be turned off at the linac (in situations discussed above), patient rotation should be determined using a spine setup plan under the clinical judgment that the PTV margin supports the additional uncertainty of the rotational accuracy. It therefore may be prudent to generate a spine setup plan (with a low prescribed dose for safety) for all fiducial based treatments.

4.5 | Correlation error

The correlation error is defined as the difference between the actual target position obtained by acquiring the live x-ray images and the position determined by the Synchrony model at that model point. The correlation errors are good indicators of the model accuracy and are displayed live during treatment (Figure 9b). The quantitative value of the error at each model point and the root mean square average over all the tracking markers of the Synchrony model are also available to the user. An excess of 5 mm in correlation error interrupts the treatment and enables the user to update or recreate the model. In clinical practice, it is recommended that the user closely monitor the correlation errors during the treatment and keep them as low as reasonably achievable. Based on previous publications, maintaining an average correlation model error of <3 mm is clinically achievable.[48]

4.6 | Uncertainty in synchrony delivery

The correlation error is the major source of error, but not the only one in Synchrony tracking. The overall Synchrony delivery accuracy depends on: (1) having an accurate model for the distribution of the target and marker positions, (2) accurately predicting future positions (~115 ms in the future), and (3) accurate system targeting (<1 mm). However, system targeting accuracy is usually not a significant source of uncertainty. Reported previously, the mechanical robot targeting inaccuracy is 0.1 mm and the maximum position uncertainty is 0.3 mm for fiducial tracking.[49] The correlation modeling and predicting accuracy have been studied by multiple investigators.[48,50,51] Hoogeman et al.[48] studied 44 lung patients with a total of 158 fractions treated. Their study showed that the residual error with Synchrony real-time respiration tracking was small (mean correlation errors are <0.3 mm). For a range of respiratory motion amplitudes up to 2 cm the intrafraction error (standard deviation of the correlation errors) was less than 2.5 mm.[48] They found that larger correlation errors were highly correlated with larger tumor motion. Pepin et al.[51] quantified the overall prediction uncertainties in the synchrony respiratory tracking system and found that margins of 1.2 mm in the lateral direction, 1.7 mm in the anterior-posterior direction, and 3.5 mm for the superior-inferior direction would provide 95% model point coverage for 95% of the population.[51] Simulation study and phantom measurement[50,52,53] showed that irregular breathing and hysteresis (phase shift) degraded the tracking accuracy. More frequent imaging and model updating was recommended for patients with irregular breathing, and dual poly modeling was found to be helpful in reducing correlation errors when hysteresis existed.[50]

The above uncertainty did not include the impact of tumor deformation and possible fiducial migration. Based on a retrospective treatment planning study on a small set of patients, Lu et al.[54] reported that if tracking is perfect, a 3 mm margin is needed to compensate for organ deformation to ensure 95% isodose coverage.[54] For soft tumor tracking with fiducials, the tracking accuracy also relies on proper fiducial positioning.[55] Fiducial placement principles and guidelines[47] should be followed, and education provided to the interventional medical staff who perform fiducial implant procedures.[56,57] Fiducials may migrate prior to or after CT simulation.[58] If the fiducials migrate after CT simulation, there is a risk of a large treatment delivery inaccuracy or tracking may not be possible at all. Therefore, it is recommended to perform simulations for soft-tissue targets where fiducials are used for tracking 1 week after fiducial placement to allow fibrosing tissue to fix the fiducials in place.[47]

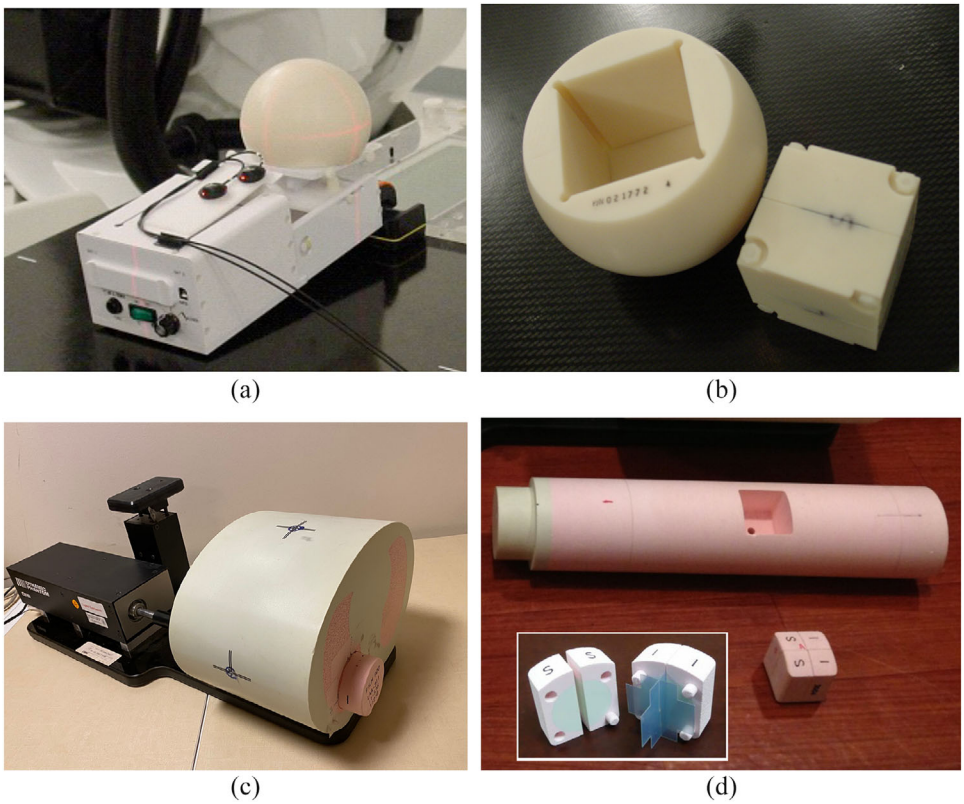

FIGURE 10 Manufacturer provided Synchrony motion platform (a) and the motion phantom (b) for QA with fiducial tracking. A commercial lung phantom (c) with a rod attached to an actuator is used for Synchrony QA with Xsight Lung tracking. The rod holds the cube with a hidden target and orthogonal radiochromic films (d).

Overall, Synchrony tracking accuracy is patient specific. A patient pre-planning study on breathing pattern, tumor motion, or a dry run of the correlation modeling may be helpful to make a decision on tumor margin.[50] Common reported margins ranged from 3 to 5 mm.[59–61] An appropriate margin should be employed to expand the clinical target volume (CTV) to planning target volume (PTV) to compensate for all possible uncertainties. The amount of margin should be determined by the physicists and the physicians based on their institutional practice.

4.7 | Synchrony QA

4.7.1 | Synchrony E2E test

While other commercial phantoms and motion platforms are also available, the manufacturer provides a Synchrony QA tool, which consists of a 12 cm diameter dome phantom that fits over the ball cube with embedded fiducials for tracking (Figure 10b).[11] This phantom assembly is placed on the motion platform (Figure 10a) that simulates the breathing cycle with motion in the superior inferior direction. An anthropomorphic phantom, known as the Xsight Lung (XLT) phantom (Figure 10c,d), manufactured by CIRS (Computerized Imaging Reference Systems, Inc.) is available for the QA of Synchrony with Xsight Lung tracking. This phantom is equipped with a radiographically equivalent lung, chest wall, spine, and ribs. A rod inserted into the lung can be moved in the S/I direction by an actuator to simulate respiratory motion. Inside the rod is a film cube with a hidden target accommodating an axial and a sagittal radiochromic film. The manufacturer's PEG[11] provides an in-depth procedure of correct setup, delivery, and analysis of the synchrony E2E tests.

Based on the collective experience of the TG members' expert consensus, the Synchrony E2E tests should be performed quarterly to ensure that the system is functional, and the tracking accuracy is within tolerance. The manufacturer's recommended tolerance for Synchrony E2E (in PEG)[11] was changed from 1.5 to 0.95 mm for the delivery software above V9.6. However, no supporting publication is available for this change. Due to the various software versions still being used clinically and that customized breathing patterns may be used in measurement, we recommend the Synchrony E2E tolerance of <0.95 mm preferred and <1.5 mm acceptable (<1.5 mm is recommended in the original TG 135).[1]

TABLE 5 Summary of QA recommendations for synchrony.

Parameter	Frequency	Tolerance	Method
E2E	Quarterly or before clinical use	Preferred: <0.95 mm Acceptable: <1.5 mm	Film in Phantom

4.8 | Summary recommendations for synchrony QC and QA

1. To create an accurate synchrony model, the LED markers should be placed near the position of maximum respiratory skin motion. For prone patients, the markers should be placed as close to the target position as the camera signal to noise ratio allows.
2. For cases with inconsistent target lock-on, burst mode should be disabled.
3. For better accuracy, an optimal synchrony model (at least eight model points) should be built before treatment starts.
4. If rotations cannot be determined (or are turned off) with the treatment plan at the linac, patient rotation should be determined using a spine setup plan according to the clinical judgment that the PTV margin supports the additional uncertainty of the rotational accuracy.
5. The average correlation error should be kept <3 mm if possible. Delivery uncertainty should be considered in the margin of PTV.
6. The Synchrony E2E test should be performed quarterly. At minimum, tolerance should be kept <1.5 mm.

A summary of recommendations for Synchrony QA is presented in Table 5.

5 | LUNG OPTIMIZED TREATMENT

5.1 | Introduction

Traditionally, CyberKnife treatment of lung tumors required the invasive placement of surrogate markers (fiducials) for tracking. Lung Optimized Treatment (LOT) is a suite of tracking solutions (called 2-view, 1-view, and 0-view tracking) for fiducial-free lung treatment that tracks the tumor directly if visible on x-rays, or indirectly using the spine if the tumor is not visible.

5.2 | Simulation CT and LOT simulation

High-resolution planning CTs (1.5-mm slice thickness or smaller is recommended) are usually acquired with patient breath hold in the supine position. LOT allows the generation of a simulation treatment plan based on a pair of normal expiration-hold CT and normal inspiration-hold CT images. However, if the image quality allows, it is preferred to extract the expiration CT and the inspiration CT from the 4D CT to generate the internal target volume (ITV), which is defined as the composite target volume expanded to include the internal tumor movement. When breath-hold CTs are to be used, it is critical to instruct the patient not to intentionally exaggerate breath-hold during the simulation to minimize both over-estimation and under-estimation of the ITV. A simulation plan is made available at the delivery workstation to check the visibility of the tumor on x-rays and to determine which tracking mode is optimal for the patient. If the 0-view or 1-view tracking mode has been identified, the pair of CT images and the delineated clinical target volumes (CTVs) are used to automatically generate the full ITV (for 0-view tracking) or the partial ITV (for 1-view tracking) in the treatment planning system. For 2-view tracking, the CTV delineated in the chosen CT (typical expiration phase/hold CT) instead of an ITV will be used for planning purposes.

5.3 | 2-view tracking

2-view tracking, also known as Xsight Lung tracking, is used when the tumor density difference from the surrounding lung tissue allows it to be identifiable in both orthogonal x-ray views. The manufacturer recommends 2-view tracking for treatment of solid tumors 1.5 cm in diameter or larger. The thickness of the chest wall may reduce tumor visibility. The tumor should not be significantly blocked by major normal structures such as the heart, vertebral bodies, and the diaphragm throughout all phases of respiration. Figure 11a,b shows a sample case.

5.4 | 1-view tracking

1-view tracking is used to track tumors that are visible in only one of the two orthogonal x-ray images. An example is shown in Figure 11c,d. The 2D information in the imaging plane (i.e., the plane orthogonal to the x-ray source-detector axis) can be extracted. Because the stereoscopic x-ray imaging system shares the superior/inferior (S/I) axis between the two imagers, the S/I component of the tumor motion can always be tracked with a single imager, which is the principal component of motion for most lung tumors.[62] The 1D information parallel to the x-ray source-detector axis cannot be identified with a single imager. This is compensated for with a

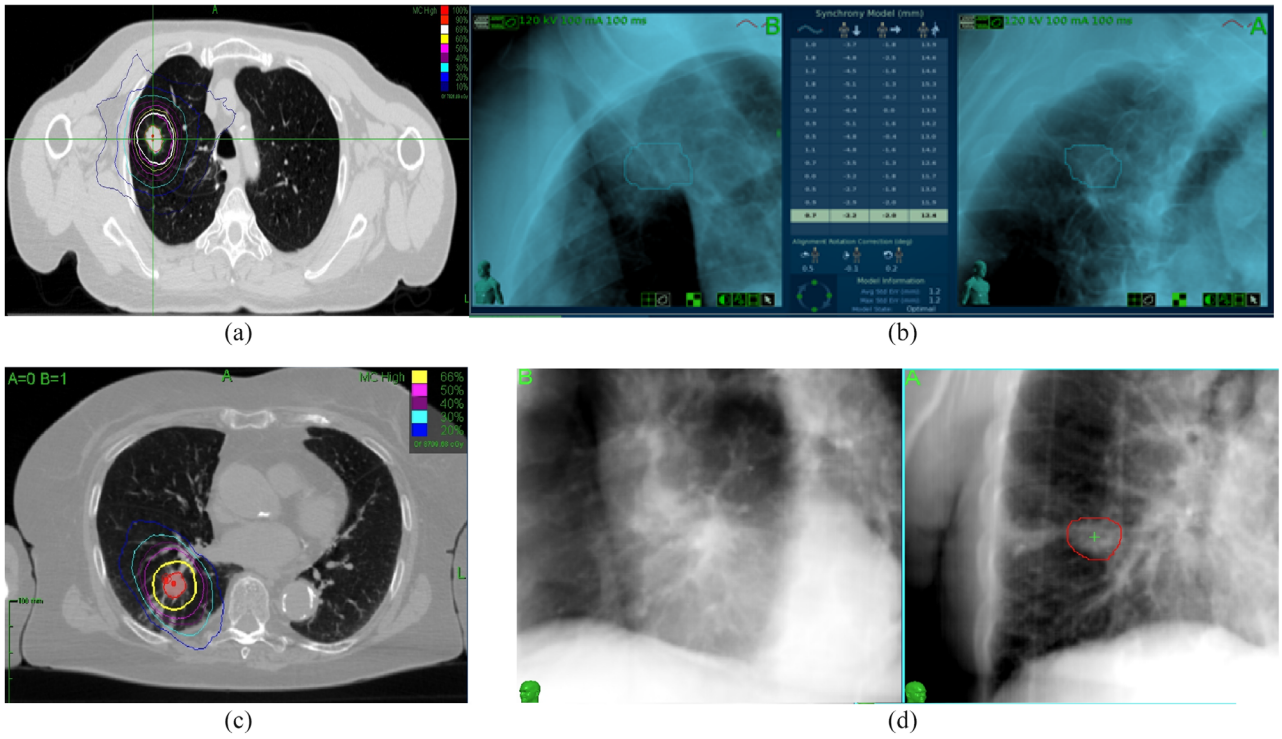

FIGURE 11 A lung tumor planned with Monte Carlo and 2-view tracking (a), and the tumor as identified in the x-ray images by the 2-view tracking LOT (b). A lung tumor planned with Monte Carlo and 1-view tracking (c), and the tumor as identified in one of the x-ray images and tracked with 1-view LOT (d).

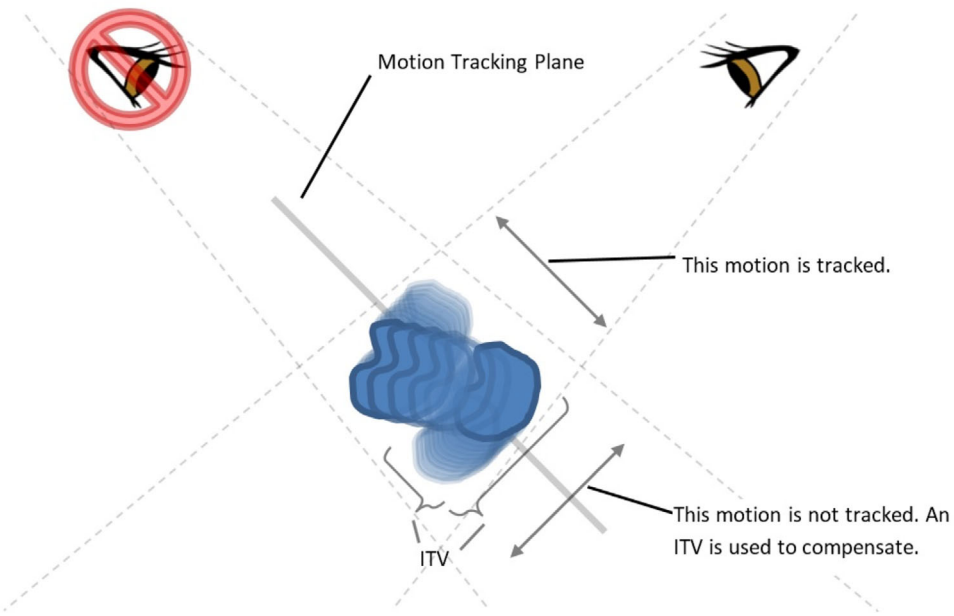

FIGURE 12 Illustration of the 1-view tracking concept. As the tumor moves through its motion trajectory (solid blue lines), the motion can be tracked from one camera view but not the other. The software generates an pITV for the untracked motion components (blue shaded areas).

partial ITV (pITV). The pITV is not a simple combination of inhale CTV and exhale CTV; rather it is an ITV determined using only the component of target motion in the untracked direction. Figure 12 illustrates the concept.

5.5 | 0-view tracking

0-view tracking uses nearby spinal skeletal structures as landmarks to treat the lung tumor. During the treatment,

rotational and translational corrections are applied to compensate for gross patient motion. The tumor motion itself is accounted for by a full ITV. The dosimetric consequences of treating an ITV for a target moving with respiration have been extensively discussed in the literature, for example, AAPM TG 76[63] and references therein. Multiple cone beam CT-based studies have found larger treatment uncertainties when the bony anatomy is used as a landmark for alignment.[64] In addition, when the tracking center is far away from the tumor, extra uncertainty is introduced due to residual angular errors.[65]

This task group does not encourage 0-view tracking treatment unless other options are not available. If used, we recommend the 0-view tracking only apply to targets with less than 1 cm respiratory motion and located less than 5 cm away from the edge of the spinal column. An appropriate margin should be used to compensate for tumor motion, estimated anatomy difference between simulation and treatment time, and additional uncertainties from angular tracking errors.[65,66]

5.6 | Tracking QA

As with other treatment modes, visual examination is essential in LOT delivery. The target outlined for tracking during the planning should be locking on the tumor in the live images. When high density objects such as bony anatomy or organs obscure the tumor in 1-view and 2-view tracking, it can be challenging for clinicians or therapists to visually check the tracking accuracy. Consequently, a quality control (QC) procedure is recommended to assist the operator in verifying tracking at every treatment. While implementation may vary between institutions, a general QC procedure is given below:

1. Appropriate education should be given to the patient not to exaggerate breathing during simulation and treatment.
2. Estimate the tumor respiratory excursion during simulation and treatment planning: The tumor respiratory shift should be determined from breath hold CTs or the 4D CT.
3. Validate the tumor expiratory position in treatment: After the patient spinal alignment, the couch shifts to the tumor region and x-ray images are acquired during expiration to allow the system to identify and "lock on" the tumor in the x-ray images. A minimal difference between the tumor location after the couch shift and where imaging locates the tumor validates that the tracking is consistent with what was planned on the primary planning (expiration) CT. A pass/fail number on this difference is beyond the scope of this report as an acceptable value would depend on the PTV margin, the surrounding structures and distance of the couch shift. It is therefore left for the user to evaluate the clinical situation and determine what is an acceptable value. It should be noted that the larger the shift between the spinal alignment and lung target, the larger the possible error that may occur due to small errors in the determination of the rotations from the spine tracking.
4. Validate the tumor excursion during treatment: Estimate the live tumor excursion from the images taken at peak (inspiration) and valley (expiration) or from the Synchrony respiratory model. The consistency between live tumor excursion and the estimated excursion during simulation and treatment planning validates the patient breathing reproducibility. We defer to each institute to develop their own threshold as the threshold (excursion inconsistency tolerance) is patient specific. It is not only proportional to the excursion of the tumor due to respiratory motion, but also could be affected by the change of the patient's breathing pattern and needs onsite clinical judgment.

Due to the complicated concepts of multiple tracking options, it is advised that the physicist be actively involved in all steps of the LOT procedures, including: patient evaluation, simulation, planning, and treatment supervision. The physicist should educate the clinical team (physician, dosimetrist, and therapist) on the concept of LOT and how to implement the QC procedure appropriately.

5.7 | QA for LOT

Physicists may use the anthropomorphic XLT phantom (Figure 10c) for 2-view, 1-view, and 0-view tracking QA by performing a phantom treatment with one of these tracking modes selected. Considering the frequency of E2E testing on Synchrony tracking and spine tracking and the fact that 2-view and 1-view shares a similar tracking algorithm, the 2-view E2E tests should be performed quarterly. The 1-view and 0-view E2E should be tested prior to clinical usage and annually thereafter. This task group recommends setting the pass criteria for the 2-view tracking E2E test to be <0.95 mm preferred, <1.5 mm acceptable.

A summary of recommendations for LOT QA is presented in Table 6.

6 | MONTE CARLO DOSE CALCULATION ALGORITHM

6.1 | Introduction

The first dose calculation available for CyberKnife plans was based on a "Ray-Tracing" algorithm, which simply

TABLE 6 Summary of QA recommendations for LOT.

LOT tracking	Frequency	Tolerance	Method
2-view E2E	Quarterly	Preferred: <0.95 mm Acceptable: <1.5 mm	Film in Phantom
1-view E2E	Prior to clinical usage and annually thereafter	Functional	Film in Phantom
0-view E2E	Prior to clinical usage and annually thereafter	Functional	Film in Phantom

employs an equivalent path length correction to account for tissue heterogeneity. While Ray-Tracing algorithms provide adequate dose calculation accuracy in water-equivalent tissue, they fail significantly in the presence of tissue heterogeneities and in low density tissue where particle disequilibrium may occur.

To improve accuracy of dose calculation, particularly in lung, Accuray Inc., with external academic collaborators,[67,68] developed a Monte Carlo (MC) algorithm which became available for fixed and Iris collimators in 2009,[69–71] and for MLC in 2017.[11] The accuracy of the MC dose calculation algorithm has been validated by different groups with measurements performed in heterogeneous slab phantoms[72–74] and comparison to independent MC dose calculations.[75] The use of an accurate dose calculation algorithm is essential in order to properly prescribe a therapeutic dose of radiation and to predict clinical outcomes.[76] It is therefore recommended that MC calculations be used for treatments of targets within or adjacent to heterogenous tissue, including air/tissue and bone tissue interfaces.[77] For NRG Oncology clinical trials (https://www.nrgoncology.org/), MC is the only approved CyberKnife treatment planning algorithm for the calculation of dose within a medium with heterogeneities. IROC (Imaging and Radiation Oncology Core) maintains a list of approved algorithms for lung treatments for all NCI sponsored clinical trials (https://irochouston.mdanderson.org/). A summary of relevant literature highlighting the need to use MC dose calculation in specific anatomical sites is reported below:

1. Lung and intrathoracic lesions: the Ray-Tracing algorithm considerably overestimates the dose delivered to the target with differences up to 33%,[78] and should not be used in these scenarios.[79–82]
2. Lesions in soft tissue and bone located in the pelvis and spine: dose calculation differences between Ray-Tracing and MC are small (within 3%) and either algorithm would produce adequate treatment plans.[70]
3. Lesions located next to large air-cavities (sinuses and nasal cavity) and spinal lesions in the thorax: Ray-Tracing might overestimate the dose to the target and MC is the preferred choice.[82,83]
4. Intracranial tumors adjacent to the skull: Ray-Tracing overestimated the target coverage with differences up to 23.5%, and MC is the preferred choice.[83,84]

In conclusion, the task group strongly recommends that MC calculations be used for lesions in the thorax (lung and thoracic spine), near air/tissue interfaces (nasal cavity), and intracranial lesions near the skull.

6.2 | Description of the MC treatment planning algorithm

To make MC practical for routine clinical dose calculation, a fast superposition MC algorithm has been implemented for CyberKnife.[85,86] A detailed description of the MC algorithm is reported in Chapter 5 (15-55) of the PEG.[11] In the following, we focus on the relevant measurements needed for each model and on clinical implications.

6.2.1 | Source model

The Monte Carlo source model is used to generate the required initial properties (position, direction, energy) of a photon incident on the patient. The source model randomly generates photons with modeled probability distribution, with each collimator having its own independent source model. All the models contain three independent components: energy spectrum, target distribution, and fluence distribution. For Iris and fixed cone, the origin (or target) and direction distributions are radially symmetric, and the energy distribution is spatially invariant. The algorithm derives the source energy distribution from the measured beam data of Percentage Depth Dose (PDD) for the largest collimator diameter of 60 mm, and the fluence distribution from one open profile (fixed collimator housing attached, and secondary collimator removed) in water (at a typical SAD = 80 cm or SSD = 80 cm and depth of 25 mm). The target distribution is derived from relative in-air output factors (OF) (all collimators) or calculated using a Gaussian distribution with a FWHM defined by the physicist. The collimation effect is included during photon sampling. Collimator sizes are not editable by the user. To account for collimator specific variations, correction factors (Collimator Correction Factors and Energy Correction Factors, which are user defined during commissioning) are introduced by the algorithm as a fine tune to the photon sampling.

For the MLC, the direction distributions are not radially symmetric. The MLC fluence distribution is calculated from the open field profiles (two orthogonal and two diagonal profiles) measured without any collimator housing attached (at a typical SAD = 80 cm or SSD = 80 cm and depth of 20 mm). The target distribution can only be calculated using a Gaussian distribution with a FWHM defined by the physicist. Different from the circular cones, the energy distribution for the MLC source model is hand-picked from a set of 11 available spectra ranging from 6.0 to 7.0 MeV. There are two sets of 11 spectra that can be toggled by selecting or unselecting the beam hardening option in the commissioning workspace. The beam hardening option should be selected to be "on" for machines with a Pb filter. M6 machines produced before April of 2017 were installed with a lead filter while the later models have the filter removed. The physicist should check with their field engineer about the filter status in order to select the right set of spectra to use.

For MLC collimation, photons are first sampled uniformly in the open field with the MLC removed, and then their weights (or probability) are modified by the fluence distribution and the MLC leaf attenuation before transporting to the patient model. The photons are attenuated by the MLC based on the location of interaction with the MLC (full leaf, leaf end, leaf end edge, leaf side edge, or not attenuated). The effect of the MLC tilt in the *Y*-direction is included in this calculation. The leaf transmission factors are pre-calculated and it is recommended not to change them during commissioning.

6.2.2 | Patient model

The patient model provides the physical material information needed for the MC transport calculations at each position within the patient, together with an external patient contour. This model is generated from the simulation CT scan, and a density model conversion table is used to convert HU numbers to mass density (1.0 g/cm^3 is water density). Note that this is different than the Ray Tracing algorithm which uses electron density. The mass density of each calculation voxel is calculated from the average CT number within the voxel. Furthermore, each voxel is assigned a material type: air, soft tissue, or bone according to the mass density in the voxel and ranges embedded in the software which cannot be edited by the user. The material type is used to define a photon Mean Free Path (MFP) at a reference density, as a function of photon energy. In the Precision system, the electron density model used for Ray-Tracing has a cut-off at −801 HU, that is, voxels corresponding to HU numbers lower than or equal to −801 are assigned an electron density equal to zero. However, there is no cut-off value for the mass density table. Voxels corresponding to HU numbers lower than −801 should be assigned linearly decreasing mass density down to 0.001 g/cm^3 (corresponding to −1000 HU). The maximum HU allowed in the table is 31 743, the maximum relative electron density value is 10 and the maximum mass density value is 22.6 g/cm^3. A detailed description of the CT density model is reported in Chapter 2 of the PEG.[11]

If possible, beams entering through metallic implants are to be avoided so that the dose calculated in the neighborhood of the target is unaffected by the implant.

6.2.3 | Beam transport and dose calculation

For the purpose of the electron transport calculations, the algorithm considers various materials as being equivalent to variable mass density water. Therefore, this algorithm calculates absorbed dose to variable-density water, which for all biological tissues, including lung and bone, is essentially equivalent to the conventional MC absorbed dose to medium as described in AAPM TG 105.[77] However, in high atomic number materials such as metallic implants, the difference between the absorbed dose to variable density water and the absorbed dose to medium calculations will be greater.

MC calculations are stochastic which means the end-result comes with a level of uncertainty at each voxel. The uncertainty is reduced by simulating more photon histories per voxel; however, this is associated with longer calculation time. The user can select the desired uncertainty at the maximum dose point to be achieved. The dose calculation uncertainty therefore increases as isodose line levels decrease, reaching 10% uncertainty or higher at the lowest isodose levels. This occurs because the number of interactions in low dose regions is lower than where the 1% uncertainty is defined. By default, the MC dose calculation treatment plan is normalized to the maximum voxel dose in the smoothed dose distribution, and the dose is calculated on the whole CT volume. The resolution of the dose calculation grid can be set to low, medium, or high. At low and medium dose grid resolution, the CT image matrix size is downscaled resulting in a faster calculation time. At high dose grid resolution, the dose is calculated in each of the CT voxels up to $512 \times 512 \times S$, where 512×512 is the CT image matrix, and S is the number of CT slices.

Typically, the final Monte Carlo simulation results are obtained with the high-resolution setting and 1% relative standard error of the mean at the maximum dose point. Calculations at lower resolution might not accurately represent the final high-resolution calculations, especially near interfaces.

6.3 | MC commissioning

6.3.1 | Commissioning procedure

During commissioning, the model refinement is through an iterative adjustment of the model parameters, by comparing calculated and measured TPR and OCR for all field sizes and depths. Due to simplification in the collimator geometry and in the dose calculated per incident history, the MC model implemented in the treatment planning system does not predict OF directly. Instead, based on the measured OF, the model generates an absolute dose normalization constant, to convert the deposited energy to the absolute dose. Therefore, it is essential to perform accurate measurements of the OF, which is particularly challenging for small fields. For guidance on small field dose measurement and corrections, this task group recommends the recently published IAEA report 483[9] (Dosimetry of small static fields used in external beam radiotherapy) and TG 155.[10] As the last step of MC commissioning, the user reviews the agreement between measured and calculated OFs and approves the MC model.

6.3.2 | Model and data agreement

During commissioning, it is recommended to set the calculation uncertainty to 0.5% for TPR and OCR, and to 0.2% for OF to reduce statistical uncertainties (PEG—Monte Carlo Commissioning Workflow).[11] The task group recommends that the agreement between measured and calculated TPR should be within 1% for all field sizes at depths of ≥15 mm. The agreement between measured and calculated OCR should be <2% in the field, and 1 mm in FWHM field size. The OF should agree with measured values within 0.5%.

While the above recommendations are achievable for most of the clinically relevant field sizes and depths, deviations larger than 2% have been observed on the shoulder and the tail regions for large field size OCRs (60 mm circular fields and larger than 60 mm MLC fields), with the discrepancy increasing with depth (≥200 mm).[11] These deviations are believed to be caused by the simplification of the MC source model (single source model) and the measurement uncertainties.

6.3.3 | Model verification

For the MC algorithm, measurements need to be performed to validate the accuracy of the model on both homogeneous and heterogeneous phantoms. Single beam QA can be done on a slab phantom containing bone and lung equivalent materials similar to the one shown in Wilcox and Daskalov.[73] The phantom is scanned, CT data transferred into the treatment planning system and a plan is calculated using a single beam. The phantom is then irradiated and the measured PDD and dose profiles are compared. The agreement between the MC calculated dose distributions and measured dose should be better than 2% on average for the entire range of collimator sizes.

6.4 | Delivery QA for diverse treatment sites

Recent reports on safety and QA for Stereotactic Radiosurgery (SRS) and Stereotactic Body Radiation Therapy (SBRT) strongly recommend a DQA process[25,26] similar to IMRT patient specific dose QA on C-arm linacs. At commissioning, it is recommended to perform an independent validation of the MC dose calculation accuracy by performing an end-to-end test through an independent review, such as the Anthropomorphic Phantoms from MD Anderson Phantom Laboratory. After MC commissioning, DQA tests for thoracic patients should be performed on a lung phantom using the MC calculation. The QA phantom used for DQA needs to be constructed such that ion chambers for point measurements and film (or other planar detectors capable of high resolution 2D dosimetry) for planar dose measurements can be inserted. Planar film can be inserted into the BallCube phantom that is designed for the CyberKnife or one of several phantom models available commercially. The DQA test using MC calculations on a lung phantom should be performed at commissioning (see Table 7). After commissioning, annual QA on the MC as part of the treatment planning system should follow AAPM TG 53[6] and MPPG 5.a/5.b [7,8] as applicable.

6.5 | Independent MU checks for MC

An independent dose calculation algorithm is often used to check the dose calculated at a reference point in a plan.[87] The independent dose calculation algorithm is usually fairly simple and based on a Clarkson integration in water-equivalent media. Therefore, the differences to MC calculations can be quite large, particularly if the area of calculation contains large distances as well as scatter volumes in non-unity density materials. The differences between typical Clarkson-based (and similar) independent calculations and the Ray-Tracing algorithm (for cones) or FSPB (for MLC) will be small because Ray-Tracing/FSPB also does not consider the scatter component of the dose and is therefore more similar to the independent calculation algorithm. To use an independent MU check algorithm based on Clarkson integration, the user has to recalculate the plan with Ray-Tracing/FSPB before exporting the beam

TABLE 7 Summary of QA recommendations for MC.

Frequency	Parameter	Tolerance	Method
Commissioning	TPR	<1%	MC calculation vs. measured dose
	OCR	<2% in field <1 mm FWHM width	MC calculation vs. measured dose
	OF	<0.5%	MC calculation vs. measured dose
	Single beam PDD and profile	<2%	Film and ion chamber in heterogeneous slab phantoms
	DQA	<5% (MPPG 5a or IROC recommendation)	Phantoms from MD Anderson Phantom Laboratory or similar phantom
Annual	Annual QA as part of the treatment planning system. Follow AAPM TG 53[6] and MPPG 5.a/5.b[7,8] as applicable.		

TABLE 8 Daily QA summary.

Report/Section	Item	Tolerance
TG 135/II.A.2	Safety Interlocks (Door, Console EMO, Key)	Functional
	CCTV cameras and monitors	Functional
	Audio monitor	Functional
	Collimator assembly collision detector	Functional
TG 135/II.B.1	Accelerator warm-up: 6000 MU for open chambers, 3000 MU for sealed chambers	N/A
	Accelerator output	>2% adjust calibration
	Detection of incorrect and missing secondary (fixed) collimator	Functional
TG 135/III.B.2	Visual check of beam laser and a standard floor mark	<1 mm
TG 135.B/3.5.3	MLC Leaf position test (Picket fence test)	Visual examination
TG 135/III.C.1 TG 135.B/2.6, 3.6	AQA test (alternate through existing collimator systems.)	<0.95 mm from baseline

list. However, the above strategy only checks system consistency, such as beam data change and system corruption. It is not a complete independent MU check on the Monte Carlo calculation algorithm. For a complete independent MU check, a calculation algorithm with similar calculation accuracy in handling tissue heterogeneities is recommended. Recently, an independent 3D dose calculation that uses a Monte Carlo algorithm and displays 3D gamma and DVH analyses on patient CT data has been developed[32] and commercial software has become available (Section 3.5.4). Agreement on the independent check is expected to be better than 5% for beams directly contributing to dose deposition at the calculation point (i.e., with off axis position smaller than the beam radius), and better than 3% on total dose at the calculation point.[88]

6.6 | Summary recommendations for MC QA

A summary of recommendations for MC QA is presented in Table 7.

7 | SUMMARY AND QA CHECKLISTS

Technological changes in robotic radiosurgery combined with maturing clinical experience and a greater record of peer-reviewed publications evaluating the technology has required an update to clinical physics QA practice. To facilitate practice change, the authors of this task group have combined the QA recommendations from the original AAPM TG 135[1] with new recommendations from this task group in the tables below. As the technology develops further, we recommend clinical physicists review the recommendations regularly based on current literature to update and adapt these QA tests to state-of-the art clinical practice. All the commissioning and ongoing QA program should be overseen by a qualified medical physicist. Information on qualifications and responsibilities of medical physicists can be found in MPPG 9.a.[27]

7.1 | Daily QA

Daily QA is summarized in Table 8. Basic daily QA on safety, laser, machine warmup, and output check remain

TABLE 9 Monthly QA summary.

Report/Section	Item	Tolerance
TG 135/ II.A.2	Safety Interlocks	Functional
TG 135/ II.B.2 TG 135.B/7.2	Energy constancy Beam symmetry Beam profile constancy: Output	<2% <3% (largest field size) <2% <2%
TG 135/ II.C.1	Imager Alignment	1 mm or center pixel ± 2 pixels
TG 135/ II.C.3	Contrast, noise, and spatial resolution of amorphous silicon detector Homogeneity/bad pixel map	To be decided by user based on available literature
TG 135/ II.D	Custom CT model: CT QA (spatial accuracy, electron density)	See AAPM TG 66[89]
TG 135/ III.B.1 TG135.B/2.3, 3.5	Verify relative location of beam laser vs. CAX, alternate through available collimators, quarterly per collimator.	Preferred: <0.5 mm Acceptable: <1.0 mm
TG 135/ III.B.2	Visually check isocentric plan to verify beam laser illuminates isocrystal; rotate through path sets each month	Laser on isocrystal for each node
TG 135.B/2.5.1, 2.5.2	Iris Field size consistency	Preferred: ±0.2 mm from baseline, Acceptable: ±0.5 mm for FS ≥ 10 mm
TG 135.B/3.5.3	MLC Leaf position test (Garden fence test)	>90% deviations < 0.5 mm, mean deviation < 0.2 mm, all < 0.95 mm
TG 135/ III.C.2 TG 135.B/ 4.7,5.7	Cover all the collimators in clinical use, schedule tracking modes on a rotational basis. Schedule LOT and Synchrony quarterly	Static E2E: < 0.95 mm Synchrony E2E: < 0.95 mm preferred, <1.5 mm acceptable
TG 135/ III.D.	Observe Synchrony treatment or simulation; listen for unusual noise and visually check for vibration	No significant change from baseline
TG 135/ III.C.3 TG 135.B/3.5.4	Non-isocentric patient QA or DQA Iris/Fixed: Monthly MLC: preferred per plan, acceptable monthly	Gamma 2% /2 mm for static (>90%) Gamma 3% /3 mm for motion tracking (>90%)

the same as in TG 135.[1] Additional QA includes MLC daily QA with film-based picket fence test and AQA test with Iris and MLC. Both testing procedures are described in detail in the PEG.[11] The film-based picket fence test is a qualitative test visually comparing the results to a baseline film.[11] AQA, a test similar to a traditional Winston Luz test, only contains an anterior and lateral beam not part of the clinical treatment paths and, therefore, is purely a system consistency check.[1,11] The task group recommends one AQA test daily (tolerance: <0.95 mm) alternating through the collimators in a week.

7.2 | Monthly QA

Monthly QA is summarized in Table 9. QA and tolerances on output and beam constancy remain the same as in TG 135[1] except that this task group recommends that beam symmetry be checked using the maximum field size available on the system. For systems with Iris and MLC collimators, Iris field size and MLC positioning QA are added (discussed in Sections 2 and 3). Monthly laser versus beam CAX check is recommended to alternate through all the collimators available or quarterly per collimator. The tolerance is <0.5 mm at 80 cm SAD preferred (as in the original TG 135[1]), and <1.0 mm at 80 cm SAD acceptable following the manufacturer's recommendation (discussed in Section 2.3).

E2E tests with Iris and MLC are included. The tests performed each month should cover all collimators in clinical use and rotate through tracking modes. We recommend using the full path for all the E2E tests. If the machine is equipped with all three collimator types, three E2E tests should be performed. An example combination is listed as: skull tracking using fixed cone, spine tracking using Iris, and fiducial tracking using MLC. This combination can be altered in the next month.

Non-isocentric DQA was recommended as periodic QA, but not clearly recommended as monthly QA in the previous TG 135.[1] In Table 9, this task group clarifies that non-isocentric DQA should be performed monthly. The selected monthly DQA cases should include Iris and fixed cones. For treatment using MLC, we recommend patient DQA for every case as a precaution at this moment and minimum monthly DQA as an acceptable alternative (Section 3.5.4). Gamma tolerance for DQA and patient DQA, as well as all other QA remains the same as in TG 135.[1]

TABLE 10 Annual QA summary.

Report/Section	Item	Tolerance
TG 135/ II.A.2	EPO button	Functional
TG 135/ II.B.3 TG 135.B/7.3	TG-51 or IAEA TRS-398, including secondary independent check	Adjust calibration if >1% difference is found
	Beam data checks on at least three field sizes *per collimator assembly*, including largest and smallest clinically relevant field size, and compared to commissioning data.	
	TPR or PDD constancy Profile constancy	<2% for FS ≤20 mm, <1% for FS > 20 mm < 2%
	Iris field size (FWHM)	Preferred: ±0.2 mm Acceptable: ±0.5 mm
	Relative OF	Preferred: <1% for FS ≥ 10 mm, <2% for FS < 10 mm (< 5% for Iris and when FS < 5 mm) Acceptable: <2% for FS ≥10 mm, <3% for FS < 10 mm (< 5% for Iris and when FS < 5 mm)
	Dose output linearity to the lowest MU used and highest clinical MU	<1%
TG 135.B/3.5.2	MLC leakage	Max transmission < 0.5%
TG 135/ II.C.2	Imager kVp accuracy, mA station exposure linearity, exposure reproducibility, focal spot size	See Table 1 in AAPM TG 135 for references
TG 135/ II.C.3	Signal to noise ratio, contrast to noise ratio, relative modulation transfer function, imager sensitivity stability, bad pixel count and pattern, uniformity corrected images, detector centering, and imager gain statistics	Compare to baseline
TG 135/ II.D TG 135.B/7.3	AAPM TG 53 and MPPG 5.a/5.b as applicable	AAPM TG 53[6], MPPG 5.a/5.b[7,8]
	CT QA (in addition to monthly tests)	AAPM TG 66 [89]
	Data security and verification	Functional
TG 135/ III.B.2	2nd Order Path Verification (including paths for all available collimators); currently only possible with the help of a service engineer. Beam laser vs. CAX must be checked to be unchanged before path verification	Preferred: Each node < 0.5 mm, RMS < 0.3 mm Acceptable: RMS < 0.5 mm
TG 135/ III.D	Check noise level of optical markers	<0.2 mm
TG 135/ IV.C	Run Synchrony E2E test with at least 20° phase shift; analyze penumbra spread	Compare to baseline
TG 135/ IV.C	Monthly QA	In addition to tolerances listed above, update all parameters and checklists
TG 135/IV.B	Daily QA	Update parameters
TG 135.B	Review all Policies & Procedures related to robotic radiosurgery	Update to current clinical practice; all team members read and sign

E2E tests with LOT/Synchrony should be scheduled quarterly as discussed in chapters 4 and 5. Quarterly laser versus field center coincidence check with Iris and MLC (<1.0 mm) is included in monthly QA summary in Table 9.

7.3 | Annual QA

Annual QA is summarized in Table 10.

The beam constancy tolerances were not provided in the previous TG 135[1] and are now provided in Table 10. The recommendations are made based on the clinical experiences of the authors of this task group (we surveyed five machines within our group), as well as the available publications.[27,40,41,23] Small field measurement is tricky and the uncertainty is highly dependent on the equipment used. Therefore, we introduced double level tolerances in some of the checks. The purpose is to encourage the best accuracy and high standard. At the same time, when the preferred recommendations are not met, instead of rushing to make hasty patches every time, the acceptable alternative can enable trending, troubleshooting, and thoughtfully planned detailed calibrations to achieve the preferred recommendations over time, to provide the best possible accuracy for every patient.

TABLE 11 Special QA after upgrades and repairs.

Report/Section	Occasion	Item	Tolerance
TG 135/ II.A.1, II.D	Software upgrade	Patient exclusion zone boundaries	Functional
		Beam data security	Functional
		HIPAA compliance procedures	Up-to-date with regulatory and institutional policies
TG 135/ II.C.1	Imager Exchange	Imager alignment, bad pixels, spatial resolution, contrast, noise, E2E	
TG 135.B/2.5.2	Iris recalibration	Field size consistency	Preferred: ±0.2 mm from baseline Acceptable: ±0.5 mm for field sizes ≥ 10 mm
TG 135.B/3.5.3	MLC recalibration	Leaf position test (Garden fence test)	>90% deviations <0.5 mm, mean deviation <0.2 mm, all <0.95 mm
TG 135.B/6.3,6.5	MC Commissioning	TPR	<1%
		OCR	<2% in field <1 mm FWHM
		OF	<0.5%
		Single beam PDD and profile	<2%
		MC DQA in heterogeneous phantom	<5%

The recommended tolerances are compared to the commissioning data. In Table 10, TPR/PDD constancy should be <1% for field size ≥20 mm and <2% for field size <20 mm; profile constancy should be <2%; output factor constancy is preferred with <1% for field sizes ≥10 mm and <2% for field sizes <10 mm (<5% for Iris 5 mm and 7.5 mm fields, and when field sizes <5 mm), and acceptable with <2% for field sizes ≥10 mm and <3% for field sizes <10 mm (<5% for Iris 5 mm and 7.5 mm fields, and when field sizes <5 mm); Iris FWHM is preferred within ±0.2 mm and acceptable within ±0.5 mm; and output linearity should be <1% within lowest MU to highest MU used clinically. FWHM for Iris should be determined from the average of the four profiles as suggested in PEG.[11] Our acceptable recommendation on energy and profile constancy mostly agree with TG 142[23] and the MPPG 8.a /MPPG 8.b[40,41] recommendations on linear accelerator performance tests. Tolerances for the relative output are tighter than the MPPG 9.a and 8.b guidelines.[27,41] While output factor constancy within 3% can be mostly achieved, occasional violations may occur for the 5 mm cone, especially at the distance of 65 cm where the actual field size is ~4 mm, and for Iris 5 and 7.5 mm fields. Therefore, we suggest 5% tolerances for those circumstances following MPPG[27,41] guidelines. Beam data constancy is highly dependent on equipment and setup consistency. For beam data measurement setup and procedures, we refer to the vendor published PEG.[11]

We also added the MLC leakage test (Section 3.5.2) to the annual checklist. Relevant checks (such as path verification and the monthly and daily QA parameters) should be automatically expanded to all the available collimators. The laser to radiation coincidence check is added as part of the annual checklist (should be performed before path calibration/verification and after laser replacement). While the PEG recommends 1 mm tolerance at 80 cm, this group prefers 0.5 mm at 80 cm especially for the fixed collimator due to the laser being used as a substitute for the radiation beam targeting (discussed in Section 2.3). PEG recommendations are adopted as minimum requirement. In addition, this task group recommends that clinical and QA policies and procedures should be reviewed annually. Treatment planning QA is not in the scope of this document. We refer to TG 53[6] (Quality assurance for clinical radiotherapy treatment planning) and MPPG 5.a/5.b.[7,8](Commissioning and QA of Treatment Planning Dose Calculations—Megavoltage Photon and Electron Beams). All other recommendations remain the same as TG 135.[1]

7.4 | Special considerations after upgrades and repairs

Special QA recommended after upgrades and repairs is summarized in Table 11. QA recommendations are also added for Iris and MLC recalibration and MC commissioning (Sections 2, 3, and 6). QA after software upgrade and imager exchange remain the same as TG 135.[1]

7.5 | QA checklists

QA checklists for daily, monthly, annual as well as the special QA after upgrades and repairs are presented in Tables 8–11.

ACKNOWLEDGMENTS

Dr. Sonja Dieterich chaired this task group prior to 2019, during the development and review of the initial version of the manuscript. The authors wish to acknowledge her leadership and invaluable contributions. The authors extend their gratitude to the AAPM Therapy Physics Committee (TPC), the Quality Assurance and Outcome Improvement Subcommittee (QASC), and the Working Group on External Beam Quality Assurance (WGEBQA) for their professional guidance and support throughout the publication process. The authors deeply appreciate the reviewers for their valuable insights, which significantly enhanced the final version of this document. Additionally, the authors thank Accuray Inc. for providing technical information on the CyberKnife robotic systems. [Correction added on 2 November, 2024 after first online publication: acknowledgment is updated.]

CONFLICT OF INTEREST STATEMENT

The Chair of the AAPM Task Group Report 135.B has reviewed the required Conflict of Interest statement on file or each member of AAPM Task Group Report 135.B and determined that disclosure of potential Conflicts of Interest is an adequate management plan.

The members of AAPM Task Group Report 135.B listed below attest that they have no potential Conflicts of Interest related to the subject matter or materials presented in this document: Lei Wang, Anand Prabhu, Ellen Wilcox, Jun Yang, Christoph Fuerweger, Jeffrey Garrett, David Taylor, Sonja Dieterich.

The members of AAPM Task Group Report 135.B listed below disclose the following potential Conflict(s) of Interest related to subject matter or materials presented in this document: Alan Cohen, Matt Noll, Martina Descovich.

Alan Cohen worked as a medical physicist at Accuray Inc. between November 2006 to June 2016. Matt Noll is currently the senior physics manager at Accuray Inc. Martina Descovich served as a member of the CyberKnife and Radixact clinical advisory boards in 2017–2018

REFERENCES

1. Dieterich S, Cavedon C, Chuang CF, et al. Report of AAPM TG 135: quality assurance for robotic radiosurgery [published online ahead of print 2011/08/06]. *Med Phys*. 2011;38(6):2914-2936.
2. Echner GG, Kilby W, Lee M, et al. The design, physical properties and clinical utility of an iris collimator for robotic radiosurgery [published online ahead of print 2009/08/19]. *Phys Med Biol*. 2009;54(18):5359-5380.
3. Fürweger C, Prins P, Coskan H, Heijmen BJ. Characteristics and performance of the first commercial multileaf collimator for a robotic radiosurgery system. *Med Phys*. 2016;43(5):2063-2071.
4. Asmerom G, Bourne D, Chappelow J, et al. The design and physical characterization of a multileaf collimator for robotic radiosurgery. *Biomed Phys Eng Express*. 2016;2(1):017003.
5. Benjamin P, Fahimian LW. Introduction to CyberKnife® Technology. In: Steven D. Chang AV, eds. *CyberKnife Stereotactic Radiosurgery*. Nova Science Publishers, Inc.; 2014:1-12.
6. Fraass B, Doppke K, Hunt M, et al. American Association of Physicists in Medicine Radiation Therapy Committee Task Group 53: quality assurance for clinical radiotherapy treatment planning [published online ahead of print 1998/11/04]. *Med Phys*. 1998;25(10):1773-1829.
7. Smilowitz JB, Das IJ, Feygelman V, et al. AAPM Medical Physics Practice Guideline 5. a. AAPM Medical Physics Practice Guideline 5.a.: commissioning and QA of treatment planning dose calculations — megavoltage photon and electron beams. *J Appl Clin Med Phys*. 2015;16(5):14-34.
8. Geurts MW, Jacqmin DJ, Jones LE, et al. AAPM Medical Physics Practice Guideline 5.b: commissioning and QA of treatment planning dose calculations-Megavoltage photon and electron beams [published online ahead of print 20220810]. *J Appl Clin Med Phys*. 2022;23(9):e13641.
9. *Dosimetry Of Small Static Fields Used In External Beam Radiotherapy*. International Atomic Energy Agency; 2017. IAEA report 483.
10. Das IJ, Francescon P, Moran JM, et al. Report of AAPM Task Group 155: megavoltage photon beam dosimetry in small fields and non-equilibrium conditions. *Med Phys*. 2021;40(10):e886-e921 doi:10.1002/mp.15030
11. *Physics Essential Guide*. Accuray Inc.; 2017.
12. Baart VDM, Lenaerts E. Validation and use of the "Iris Quality Assurance Tool". Paper presented at: SRS/SBRT RSS Scientific Meeting; 2013; Carlsbad, CA.
13. Jr TD. Evaluation of a prototype optical image-based measurement tool for routine quality assurance of field size for the CyberKnifeTM IRIS collimation system. Paper presented at: SRS/SBRT RSS Scientific Meeting; 2012; Carlsbad, CA.
14. Nikolic M, Masterson-McGary M, Toner S, et al. MO-D-105-06: dose-area product as a method for small field geometric QA. *Med Phys*. 2013;40(6):395-395.
15. Heidorn S-C, Kremer N, Fürweger C. A novel method for quality assurance of the cyberknife iris variable aperture collimator. *Cureus*. 2016;8(5):e618.
16. Wang AL L, Ho A. Implementation of the electronic portal imaging device for dailycyberknife quality assurance. *Med Phys*. 2018;45(6):e327. SU-I-GPD-T-380.
17. Ashraf MR, Gibson C, Skinner L, Gu X, Xing L, Wang L. An integrated 3D printed radioluminescent-based phantom for quality assurance on a robotic-arm linac. *Phys Med Biol*. 2023;68:115003. doi:10.1088/1361-6560/acd162
18. Burton SHD, Huq MS. Dosimetric comparison between cone/Iris-based and InCise MLC-based CyberKnife plans for single and multiple brain metastases. *J Appl Clin Med Phys*. 2016;17(5):184-199.
19. Kathriarachchi V, Shang C, Evans G, Leventouri T, Kalantzis G. Dosimetric and radiobiological comparison of CyberKnife M6 InCise multileaf collimator over IRIS variable collimator in prostate stereotactic body radiation therapy. *J Med Phys*. 2016;41(2):135-143.
20. McGuinness CMGA, Lessard E, Nakamura JL, et al. Investigating the clinical advantages of a robotic linac equipped with a multileaf collimator in the treatment of brain and prostate cancer patients. *J Appl Clin Med Phys*. 2015;16(5):284-295.
21. Bayouth JE, Wendt D, Morrill SM. MLC quality assurance techniques for IMRT applications [published online ahead of print 2003/05/30]. *Med Phys*. 2003;30(5):743-750.
22. Arthur Boyer PD, Peter Biggs PD, James Galvin DS, et al. AAPM TG-50: Basic Applications Of Multileaf Collimators. *American Asociation of Physicists in Medicine*; 2001.
23. Klein EE, Hanley J, Bayouth J, et al. Task Group 142 report: quality assurance of medical accelerators [published online ahead of print 2009/10/09]. *Med Phys*. 2009;36(9):4197-4212.

24. Murphy MJ, Cox RS. The accuracy of dose localization for an image-guided frameless radiosurgery system [published online ahead of print 1996/12/01]. *Med Phys*. 1996;23(12):2043-2049.
25. Benedict SH, Yenice KM, Followill D, et al. Stereotactic body radiation therapy: the report of AAPM Task Group 101 [published online ahead of print 2010/10/01]. *Med Phys*. 2010;37(8):4078-4101.
26. Solberg TD, Balter JM, Benedict SH, et al. Quality and safety considerations in stereotactic radiosurgery and stereotactic body radiation therapy: executive summary [published online ahead of print 2012/01/01]. *Pract Radiat Oncol*. 2012;2(1):2-9.
27. Halvorsen PH, Cirino E, Das IJ, et al. AAPM-RSS medical physics practice guideline 9.a. for SRS-SBRT [published online ahead of print 2017/08/09]. *J Appl Clin Med Phys*. 2017;18(5):10-21.
28. Ford EC, Terezakis S, Souranis A, Harris K, Gay H, Mutic S. Quality control quantification (QCQ): a tool to measure the value of quality control checks in radiation oncology. *Int J Radiat Oncol*Biol*Phys*. 2012;84(3):e263-e269.
29. Bojechko C, Phillps M, Kalet A, Ford EC. A quantification of the effectiveness of EPID dosimetry and software-based plan verification systems in detecting incidents in radiotherapy. *Med Phys*. 2015;42(9):5363-5369.
30. Kry SF, Molineu A, Kerns JR, et al. Institutional patient-specific IMRT QA does not predict unacceptable plan delivery. *Int J Radiat Oncol* Biol* Phys*. 2014;90(5):1195-1201.
31. Kry SF, Glenn MC, Peterson CB, et al. Independent recalculation outperforms traditional measurement-based IMRT QA methods in detecting unacceptable plans. *Med Phys*. 2019;46(8):3700-3708.
32. Milder MTWAM, Söhn M, Hoogeman MS. Commissioning and clinical implementation of the first commercial independent Monte Carlo 3D dose calculation to replace CyberKnife M6™ patient-specific QA measurements. *J Appl Clin Med Phys*. 2020;21(11):304-311. doi:10.1002/acm2.13046
33. Miften M, Olch A, Mihailidis D, et al. Tolerance limits and methodologies for IMRT measurement-based verification QA: recommendations of AAPM Task Group No. 218 [published online ahead of print 2018/02/15]. *Med Phys*. 2018;45(4):e53-e83.
34. Blanck O, Masi L, Damme MC, et al. Film-based delivery quality assurance for robotic radiosurgery: commissioning and validation. *Eur J Med Phys*. 2015;31(5):476-483.
35. Lin MH, Veltchev I, Koren S, Ma C, Li J. Robotic radiosurgery system patient-specific QA for extracranial treatments using the planar ion chamber array and the cylindrical diode array. *J Appl Clin Med Phys*. 2015;16(4):290-305.
36. Blanck O, Masi L, Chan MK, et al. High resolution ion chamber array delivery quality assurance for robotic radiosurgery: commissioning and validation. *Phys Med*. 2016;32(6):838-846.
37. Rose MS, Tirpak L, Van Casteren K, et al. Multi-institution validation of a new high spatial resolution diode array for SRS and SBRT plan pretreatment quality assurance [published online ahead of print 2020/03/28]. *Med Phys*. 2020;47(7):3153-3164.
38. Padelli FAD, Fariselli L, De Martin E. IBA myQA SRS detector for CyberKnife robotic radiosurgery quality assurance. *Appl Sci*. 2022;12(15):7791.
39. Ashraf MR, Krimmer J, Zalavri L, Gu X, Wang L, Chuang CF. Angular correction methodology and characterization of a high-resolution CMOS array for patient specific quality assurance on a robotic arm linac [published online ahead of print 20230802]. *J Appl Clin Med Phys*. 2023;24(11):e14110.
40. Smith K, Balter P, Duhon J, et al. AAPM Medical Physics Practice Guideline 8.a.: linear accelerator performance tests [published online ahead of print 2017/05/27]. *J Appl Clin Med Phys*. 2017;18(4):23-39.
41. Krauss RF, Balik S, Cirino ET, et al. AAPM Medical Physics Practice Guideline 8.b: linear accelerator performance tests [published online ahead of print 20231004]. *J Appl Clin Med Phys*. 2023;24(11):e14160.
42. Schweikard A, Shiomi H, Adler J. Respiration tracking in radiosurgery. *Med Phys*. 2004;31(10):2738-2741.
43. Dieterich S. Dynamic tracking of moving tumors in stereotactic radiosurgery. In: Mould RF, ed. *Robotic Radiosurgery*. The CyberKnife Society Press; 2005:51-63.
44. Dieterich S, Cleary K, D'Souza W, Murphy M, Wong KH, Keall P. Locating and targeting moving tumors with radiation beams [published online ahead of print 2009/01/30]. *Med Phys*. 2008;35(12):5684-5694.
45. Dieterich S, Gibbs IC. The cyberknife in clinical use: current roles, future expectations [published online ahead of print 2011/06/01]. *Front Radiat Ther Oncol*. 2011;43:181-194.
46. Fürweger C, Drexler C, Muacevic A, Wowra B, Klerck EC, Hoogeman MS. CyberKnife robotic spinal radiosurgery in prone position: dosimetric advantage due to posterior radiation access?. *J Appl Clin Med Phys*. 2014;15(4):11-21.
47. *CyberKnife Treatment Delivery System,* Version 11.1.X. Accuray Inc.; 2017.
48. Hoogeman M, Prevost JB, Nuyttens J, Poll J, Levendag P, Heijmen B. Clinical accuracy of the respiratory tumor tracking system of the cyberknife: assessment by analysis of log files [published online ahead of print 2009/04/14]. *Int J Radiat Oncol Biol Phys*. 2009;74(1):297-303.
49. Antypas C, Pantelis E. Performance evaluation of a CyberKnife G4 image-guided robotic stereotactic radiosurgery system [published online ahead of print 2008/08/13]. *Phys Med Biol*. 2008;53(17):4697-4718.
50. Seppenwoolde Y, Berbeco RI, Nishioka S, Shirato H, Heijmen B. Accuracy of tumor motion compensation algorithm from a robotic respiratory tracking system: a simulation study [published online ahead of print 2007/09/08]. *Med Phys*. 2007;34(7):2774-2784.
51. Pepin EW, Wu H, Zhang Y, Lord B. Correlation and prediction uncertainties in the cyberknife synchrony respiratory tracking system [published online ahead of print 2011/08/24]. *Med Phys*. 2011;38(7):4036-4044.
52. Akino Y, Shiomi H, Sumida I, et al. Impacts of respiratory phase shifts on motion-tracking accuracy of the CyberKnife Synchrony Respiratory Tracking System [published online ahead of print 2019/04/04]. *Med Phys*. 2019;46(9):3757-3766.
53. Marants R, Vandervoort E, Cygler JE. Evaluation of the 4D RADPOS dosimetry system for dose and position quality assurance of CyberKnife [published online ahead of print 2018/07/26]. *Med Phys*. 2018;45(9):4030-4044. doi:10.1002/mp.13102
54. Lu XQ, Shanmugham LN, Mahadevan A, et al. Organ deformation and dose coverage in robotic respiratory-tracking radiotherapy. *Int J Radiat Oncol Biol Phys*. 2008;71(1):281-289.
55. Murphy MJ. Fiducial-based targeting accuracy for external-beam radiotherapy. *Med Phys*. 2002;29(3):334-344.
56. Kothary N, Dieterich S, Louie JD, Koong AC, Hofmann LV, Sze DY. A primer on image-guided radiation therapy for the interventional radiologist [published online ahead of print 2009/06/02]. *J Vasc Interv Radiol*. 2009;20(7):859-862.
57. Kothary N, Dieterich S, Louie JD, Chang DT, Hofmann LV, Sze DY. Percutaneous implantation of fiducial markers for imaging-guided radiation therapy [published online ahead of print 2009/03/24]. *AJR Am J Roentgenol*. 2009;192(4):1090-1096.
58. van der Voort van Zyp NC, Hoogeman MS, van de Water S, et al. Stability of markers used for real-time tumor tracking after percutaneous intrapulmonary placement [published online ahead of print 2011/02/26]. *Int J Radiat Oncol Biol Phys*. 2011;81(3):e75-81.
59. Collins BT, Vahdat S, Erickson K, et al. Radical cyberknife radiosurgery with tumor tracking: an effective treatment for inoperable small peripheral stage I non-small cell lung cancer [published online ahead of print 2009/01/20]. *J Hematol Oncol*. 2009;2:1.
60. van der Voort van Zyp NC, Prevost JB, Hoogeman MS, et al. Stereotactic radiotherapy with real-time tumor tracking for non-

small cell lung cancer: clinical outcome [published online ahead of print 2009/03/20]. *Radiother Oncol*. 2009;91(3):296-300.
61. Brown WT, Wu X, Fowler JF, et al. Fowler. *South Med J*. 2008;101:376-382.
62. Shirato H, Seppenwoolde Y, Kitamura K, Onimura R, Shimizu S. Intrafractional tumor motion: lung and liver. *Semin Radiat Oncol*. 2004;14(1):10-18.
63. Keall PJ, Mageras GS, Balter JM, et al. The management of respiratory motion in radiation oncology report of AAPM Task Group 76 [published online ahead of print 2006/11/09]. *Med Phys*. 2006;33(10):3874-3900.
64. Guckenberger M, Meyer J, Wilbert J, et al. Cone-beam CT based image-guidance for extracranial stereotactic radiotherapy of intrapulmonary tumors. *Acta Oncol*. 2006;45(7):897-906.
65. CS JJ, Lynch B, Wang B, Dunlap NE. Quantification of planning target volume margin when using a robotic radiosurgery system to treat lung tumors with spine tracking. *Pract Radiat Oncol*. 2015;5(4):e337-e343.
66. Guo Y, Zhuang H, Zhao L, Yuan Z, Wang P. Influence of different image-guided tracking methods upon the local efficacy of CyberKnife treatment in lung tumors. *Thorac Cancer*. 2015;6(3):255-259.
67. Deng J, Ma CM, Hai J, Nath R. Commissioning 6 MV photon beams of a stereotactic radiosurgery system for Monte Carlo treatment planning [published online ahead of print 2004/01/10]. *Med Phys*. 2003;30(12):3124-3134.
68. Deng J, Guerrero T, Ma CM, Nath R. Modelling 6 MV photon beams of a stereotactic radiosurgery system for Monte Carlo treatment planning [published online ahead of print 2004/05/22]. *Phys Med Biol*. 2004;49(9):1689-1704.
69. van der Voort van Zyp NC, Hoogeman MS, van de Water S, et al. Clinical introduction of Monte Carlo treatment planning: a different prescription dose for non-small cell lung cancer according to tumor location and size [published online ahead of print 2010/05/01]. *Radiother Oncol*. 2010;96(1):55-60.
70. Wilcox EE, Daskalov GM, Lincoln H. Stereotactic radiosurgery-radiotherapy: should Monte Carlo treatment planning be used for all sites?. *Pract Radiat Oncol*. 2011;1(1):251-260.
71. Wilcox EE, Daskalov GM, Lincoln H, Shumway RC, Kaplan BM, Colasanto JM. Comparison of planned dose distributions calculated by Monte Carlo and Ray-Trace algorithms for the treatment of lung tumors with cyberknife: a preliminary study in 33 patients [published online ahead of print 2009/12/17]. *Int J Radiat Oncol Biol Phys*. 2010;77(1):277-284.
72. Sharma S, Ott J, Williams J, Dickow D. Dose calculation accuracy of the Monte Carlo algorithm for CyberKnife compared with other commercially available dose calculation algorithms [published online ahead of print 2010/12/15]. *Med Dosim*. 2011;36(4):347-350.
73. Wilcox EE, Daskalov GM. Accuracy of dose measurements and calculations within and beyond heterogeneous tissues for 6 MV photon fields smaller than 4 cm produced by Cyberknife [published online ahead of print 2008/07/25]. *Med Phys*. 2008;35(6):2259-2266.
74. Heidorn SC, Kilby W, Furweger C. Novel Monte Carlo dose calculation algorithm for robotic radiosurgery with multi leaf collimator: dosimetric evaluation [published online ahead of print 2018/11/26]. *Phys Med*. 2018;55:25-32.
75. Mackeprang PH, Vuong D, Volken W, et al. Benchmarking Monte-Carlo dose calculation for MLC CyberKnife treatments. *Radiat Oncol*. 2019;14(1):172.
76. Papanikolaou N, Battista J, Boyer AL, et al. AAPM Report No. 85 : Tissue Inhomogeneity Corrections For Megavoltage Photon Beams. American Association of Physicists in Medicine by Medical Physics; 2004.
77. Chetty IJ, Curran B, Cygler JE, et al. Report of the AAPM Task Group No. 105: issues associated with clinical implementation of Monte Carlo-based photon and electron external beam treatment planning [published online ahead of print 2008/01/17]. *Med Phys*. 2007;34(12):4818-4853.
78. Braunstein SE, Dionisio SA, Lometti MW, et al. Evaluation of Ray Tracing and Monte Carlo algorithms in dose calculation and clinical outcomes for robotic stereotactic body radiotherapy of lung cancers. *J Radiosurg SBRT*. 2014;3:67-79.
79. Wu VW, Tam KW, Tong SM. Evaluation of the influence of tumor location and size on the difference of dose calculation between Ray Tracing algorithm and Fast Monte Carlo algorithm in stereotactic body radiotherapy of non-small cell lung cancer using CyberKnife [published online ahead of print 2013/09/17]. *J Appl Clin Med Phys*. 2013;14(5):68-78.
80. Latifi K, Oliver J, Baker R, et al. Study of 201 non-small cell lung cancer patients given stereotactic ablative radiation therapy shows local control dependence on dose calculation algorithm [published online ahead of print 2014/02/18]. *Int J Radiat Oncol Biol Phys*. 2014;88(5):1108-1113.
81. Liu MB, Eclov NC, Trakul N, et al. Clinical impact of dose overestimation by effective path length calculation in stereotactic ablative radiation therapy of lung tumors. *Pract Radiat Oncol*. 2013;3(4):294-300.
82. Okoye CC, Patel RB, Hasan S, et al. Comparison of ray tracing and monte carlo calculation algorithms for thoracic spine lesions treated with cyberknife-based stereotactic body radiation therapy. *Technol Cancer Res Treat*. 2016;15(1):196-202. doi:10.1177/1533034614568026
83. Wang EF L, Hayes S, Jin L, Ma C. Is Monte Carlo dose calculation method necessary for cyberknife brain treatment planning?. *Med Phys*. 2014;41(6):275.
84. Hawksworth SA, Qureshi MM, Xlang H, et al. Ray-Trace is inferior to Monte Carlo dose calculation algorithm for intracranial robotic radiosurgical treatment: a comparative dosimetry study. *Int J Radiat Oncol*. 2011;81(2):S859.
85. Ma C-M, Li JS, Deng J, Fan J. Implementation of Monte Carlo dose calculation for cyberKnife treatment planning. *J Phys Conf Ser*. 2008;102. doi:10.1088/1742-6596/102/1/012016
86. Keall PJ, Hoban PW. Superposition dose calculation incorporating Monte Carlo generated electron track kernels [published online ahead of print 1996/04/01]. *Med Phys*. 1996;23(4):479-485.
87. Stern RL, Heaton R, Fraser MW, et al. Verification of monitor unit calculations for non-IMRT clinical radiotherapy: report of AAPM Task Group 114. *Med Phys*. 2011;38(1):504-530.
88. Zhu TC, Stathakis S, Clark JR, et al. Report of AAPM Task Group 219 on independent calculation-based dose/MU verification for IMRT. *Med Phys*. 2021;48(10):e808-e829. doi:10.1002/mp.15069
89. Mutic S, Palta JR, Butker EK, et al. Quality assurance for computed-tomography simulators and the computed-tomography-simulation process: report of the AAPM Radiation Therapy Committee Task Group No. 66 [published online ahead of print 2003/11/05]. *Med Phys*. 2003;30(10):2762-2792.

How to cite this article: Wang L, Descovich M, Wilcox EE, et al. AAPM task group report 135.B: Quality assurance for robotic radiosurgery. *Med Phys*. 2024;1-32.
https://doi.org/10.1002/mp.17478